Concurrent response and action effect representations across the somatomotor cortices during novel task preparation.

Ana F. Palenciano*[1], Carlos González-García[1], Jan De Houwer[2], Baptist Liefooghe[3], and Marcel Brass[4,5]

[1] Mind, Brain and Behavior Research Center, University of Granada, 18071, Granada, Spain

[2] Department of Experimental Clinical and Health Psychology, Ghent University, 9000, Ghent, Belgium

[3] Department of Psychology, Utrecht University, 3508, Utrech, The Netherlands

[4] Berlin School of Mind and Brain, Department of Psychology, Humboldt University of Berlin, 10117, Berlin, Germany

[5] Department of Experimental Psychology, Ghent University, 9000, Ghent, Belgium

**Corresponding author.* E-mail address: palencianoap@ugr.es (Ana F. Palenciano)

Abbreviated tittle: Response and action effect coding for novel tasks.

Number of pages: 62

Number of figures: 7 figures, 6 extended data figures/tables.

Number of words: abstract, 250; introduction, 679; discussion, 1589.

Conflict of interest statement: The authors declare no competing financial interests.

Acknowledgment: This research was supported by grant G00951N of the Flemish Government attributed to BL and JDH. AFP was supported by Grant PAIDI21_00207 of the Andalusian Autonomic Government. CG-G was supported by Grant IJC2019-040208-I and Project PID2020-116342GA-I00 funded by MCIN/AEI/10.13039/501100011033, and Grant

RYC2021-033536-I funded by MCIN/AEI/10.13039/501100011033 and by the European Union NextGeneration EU/PRTR. JDH was supported by Methusalem funding from the Special Research Fund (BOF) of Ghent University (reference number: BOF22/MET_V/002). MB was supported by an Einstein Strategic Professorship of the Einstein Foundation Berlin (EPP-2018-483) and by the Deutsche Forschungsgemeinschaft (DFG, German Research Foundation) under Germany's Excellence Strategy – EXC 2002/1 "Science of Intelligence" (project number: 390523135). BL was supported by the Utrecht University Focus Area on Human-Centered Artificial Intelligence.

Abstract

Instructions allow us to fulfill novel and complex tasks on the first try. This skill has been linked to preparatory brain signals that encode upcoming demands in advance, facilitating novel performance. To deepen insight into these processes, we aimed to explore whether instructions pre-activated task-relevant motoric and perceptual neural states. Critically, we addressed whether these representations anticipated activity patterns guiding overt sensorimotor processing, which could reflect that internally simulating the novel task facilitates the preparation. To do so, we collected functional magnetic resonance imaging data while participants encoded and implemented novel stimulus-response associations. Participants also completed localizer tasks designed to isolate the neural representations of the mappings-relevant motor responses, perceptual consequences, and stimulus categories. Using canonical template tracking, we identified whether and where these sensorimotor representations were pre-activated. We found that response-related templates were encoded in advance in regions linked with action control, entailing not only the instructed responses but also their somatosensory consequences. This result was particularly robust in primary motor and somatosensory cortices. While, following our predictions, we found a systematic decrease in the irrelevant stimulus templates' representational strength compared to the relevant ones, this difference was due to below-zero estimates linked to the irrelevant category activity patterns. Overall, our findings reflect that instruction processing relies on the sensorimotor cortices to anticipate motoric and kinesthetic representations of prospective action plans, suggesting the engagement of motor imagery during novel task preparation. More generally, they stress that the somatomotor system could participate with higher-level frontoparietal regions during anticipatory task control.

Keywords: *Novel instructed behavior, cognitive control, task preparation, fMRI, multivariate analyses*

Significance Statement

By using instructions, humans can successfully implement novel stimulus-response mapping on the first try. Here, we investigated whether this skill entailed anticipating the mappings-relevant motoric and perceptual neural states before task execution. Using tailored pattern analyses and localizer tasks, we isolated a series of task-relevant sensorimotor neural representations and addressed whether they were pre-activated during novel mapping preparation. We found widespread anticipation of the response-related activity patterns, which not only entailed the relevant motor responses but also their perceptual consequences. This finding was particularly robust in primary somatomotor areas. Overall, our results stress the contribution of lower-level cortices during instructed performance, suggesting that when no experience with a task is available, simulating the prospective sensorimotor processing may facilitate optimal preparation.

1 Introduction

By using symbolic information, humans convey and communicate task procedures that they have never implemented before. Thanks to this ability, we can acquire novel and arbitrary stimulus-response (S-R) mappings directly from instructions, highlighting the adaptability of human learning processes. This complex skill has been associated with anticipatory brain signals across a set of frontal and parietal areas (Cole et al., 2010; Demanet et al., 2016; Dumontheil et al., 2011; Hartstra et al., 2011, 2012; Palenciano, González-García, Arco, & Ruz, 2019; Ruge & Wolfensteller, 2010) that overlaps with the Multiple Demand Network (MDN; Duncan, 2010; Fedorenko et al., 2013), a system linked to cognitive control. These areas encode in advance behaviorally relevant instruction information, such as the targeted stimuli, the relevant responses, or the rules binding both (Cole, Reynolds, et al., 2013; González-García et al., 2017, 2021; Muhle-Karbe et al., 2017; Palenciano, González-García, Arco, Pessoa, et al., 2019). Accordingly, current models emphasize the role of the MDN in assembling novel task representations from instructions (Brass et al., 2017; Cole, Laurent, et al., 2013). Critically, these representations are characterized by their abstract, multidimensional nature (Bourguignon et al., 2018; Cole et al., 2011; Palenciano, González-García, Arco, Pessoa, et al., 2019). How this higher-order task coding ultimately shapes the downstream sensorimotor processing and impacts instruction implementation remains elusive to date.

To address this issue, we aimed to investigate the contribution of lower-level, sensorimotor neural representations to novel task preparation. In this regard, it has been suggested that internally simulating novel tasks through imagery may facilitate optimal preparation (Moran & O'Shea, 2020). This view, based on frameworks like the motor simulation theory (Jeannerod, 1994, 2001), emphasizes that imagery is driven by an internal replay engaging action representations shared with overt performance (Grush, 2004; Guillot & Collet, 2005;

Hardwick et al., 2018). Hence, by means of imagery, novel instructions could pre-activate sensorimotor neural states overlapping with those driving task execution. Such a mechanism would bridge the above-described abstract task coding found in the MDN with the later behavioral performance. It would also be in line with more general findings from the action preparation domain, where it has been suggested that the motor system anticipates execution-induced neural states during planning (Ariani et al., 2022; Churchland et al., 2010; Shenoy et al., 2013).

Previous behavioral results have evidenced an association between novel task implementation and imagery (Liefooghe et al., 2021; Theeuwes et al., 2018). Robust evidence also emphasizes that just encoding instructions induces automatic response activation before task execution (Liefooghe et al., 2012, 2013; Liefooghe & De Houwer, 2018; Meiran et al., 2015a; Meiran & Cohen-Kdoshay, 2012). Moreover, imposing secondary motor demands during instruction preparation disrupts execution in an effector-specific fashion (Palenciano et al., 2021), suggesting that optimal anticipatory control may rely on task-relevant response representations. At the neural level, functional magnetic resonance imaging (fMRI) data have shown heightened mean activity across motor regions during instruction encoding and preparation (Hartstra et al., 2011, 2012; Ruge & Wolfensteller, 2010). Electroencephalography findings have also evidenced that instructions elicit neurophysiological signatures of response pre-activation (Everaert et al., 2014; Meiran et al., 2015a), namely, lateralized readiness potentials (Gratton et al., 1988). Nonetheless, although all these results converge on the relevance of lower-level motoric processes for novel task preparation, the underlying neural computations have not been systematically explored.

To fill this gap, we addressed whether encoding instructions pre-activated motoric and perceptual neural representations that share content and format with those involved during

sensorimotor processing. To do so, we collected fMRI data while participants encoded and executed pairs of novel S-R mappings. Then, they completed a series of localizer tasks seeking to isolate the neural activity patterns of three mappings' components: the effector-specific motor responses, their somatosensory consequences, and the targeted stimulus categories. Employing canonical template tracking (Palenciano et al., 2022), we estimated standard neural representations (or templates) from the localizer task data and assessed their representational strength during the S-R mapping paradigm. Our main prediction was that the mappings-relevant sensorimotor templates would be anticipatorily encoded in a set of regions of interest (ROIs) located across the motor, somatosensory, and visual brain systems.

2 Materials and methods

2.1. Participants

Thirty-five participants completed the experiment (27 women, 8 men; mean age = 23 years, *SD* = 3 years). All of them were right-handed, with normal or corrected-to-normal vision, and MRI compatible. Most of the participants were native Dutch speakers (N = 33), except two of them, who were fluent English speakers. All of them signed a consent form approved by the UZ Ghent Ethics Committee. The participation was compensated with 36.25 EURO. The data of four participants were discarded due to excessive movement. Another participant was unable to finish the MRI session. The data of the remaining 30 participants were included in all the analyses, with the exception of the Action Effects analysis (see Section 2.6), where data from three additional participants needed to be excluded due to technical issues with the tactile stimulators.

2.2. Apparatus, stimuli, and protocol

Novel S-R mapping paradigm

In the main paradigm, participants encoded pairs of novel S-R mappings to later implement one of them upon target presentation. For that purpose, we generated a pool of unique associations, all consisting of a picture of an animal, and a verbal label indicating the response linked to that stimulus. The mappings' response involved either the left index, the left middle, the right index, or the right middle finger. The response labels were presented either in Dutch ("*L wijs*", "*L middel*", "*R wijs*", "*R middel*") or in English ("*L index*", "*L middle*", "*R index*", "*R middle*") depending on the participant's preferred language, and were shown in font Arial, size 50 (approx. 1.2º by 3.8º). The pictures were obtained from a previous database containing 770 animate images (Brady et al., 2013; Brodeur et al., 2014; Griffin et al., 2007; Konkle et al., 2010) and completed with stimuli from the Animal Images Database (Possidónio et al., 2019), the C.A.R.E. database (Russo et al., 2018) and available sources with Creative Commons license. All the stimuli were resized to 200 by 200 pixels (approx. 4.8º), and appeared on greyscale, with the background removed and the animal centered on the canvas. Four animal categories were used: canines, felines, birds, and sea animals. For each mapping, we displayed the picture on the left side of the screen, and the response label, on the right side. In each trial, two mappings were shown, one in the upper part of the screen, and another on the lower part.

For each participant, we created a pool of 640 different S-R mappings, arranged in 320 pairs. In each trial, two out of the four possible responses and two out of the four possible animal categories were used. We ensured an equal representation of the six pair-wise responses combination ([left index, left middle], [left index, right index], [left index, right middle], [left middle, right index], [left middle, right middle], and [right index, right middle]) and the six pair-wise combinations of stimulus categories ([cat, dog], [cat, bird], [cat, fish],

165 [dog, bird], [dog, fish], and [bird, fish]). We further controlled the mappings among response
166 and stimulus pairs (i.e.: trials with [cat-left index / dog right-middle] were equally frequent as
167 trials with [bird-left middle / fish-right index]), to avoid that some categories were more
168 frequently linked to some responses by chance. The location of the mappings on the screen
169 (upper or lower part) was also counterbalanced across category and response conditions.

170 The sequence of events within a trial is depicted in **Fig. 1A**. First, the participants encoded
171 the mappings during 2s, followed by a preparation interval displaying a fixation cross, and
172 with a jittered duration (mean = 2.39s, SD = 1.26s, range = [0.6, 5s], values extracted from
173 a pseudo-logarithmic distribution). Then, a probe stimulus was presented during a window
174 of 1.75s where participants responded. In 90% of the trials, probes corresponded either to
175 the upper or the lower mapping picture (with a 50% probability each). In the remaining 10%
176 of trials (*catch trials*), a novel picture – not in any of the two mappings – was presented, and
177 participants were asked to respond with the left and right index and middle fingers
178 simultaneously. Catch trials were included to ensure that both S-R mappings were equally
179 well encoded. Catch probes were also animal pictures but always belonged to one of the
180 two categories that were not shown in the current mappings. Finally, a fixation was
181 presented during a jittered inter-trial interval (ITI), with the same temporal properties as the
182 previous one.

183 Before the MRI session, participants practiced the S-R mapping task until they achieved an
184 85% of accuracy. To ensure that the mappings from the practice session were not further
185 employed, we used a different set of stimuli composed of inanimate items (musical
186 instruments and vehicles). The stimuli from the practice session were not further employed
187 in the experiment. Once inside the MRI scanner, participants completed four task runs, each
188 containing 80 trials. They could take a self-paced pause between runs. Overall, the duration
189 of the S-R mapping task was approximately 45 minutes.

Localizer tasks

After completing the main paradigm, the participants remained on the scanner and completed three localizer tasks, designed to isolate the representations of the mappings' motor response, their somatosensory consequences, and stimulus categories. The localizers' experimental design aimed to maximize the similarity between the targeted component and the S-R mapping paradigm while keeping the remaining task features as independent as possible. This was done to avoid confounding specific template activation with more general motoric or perceptual processes (Palenciano et al., 2023). Each localizer block lasted approximately 5 minutes, and the order in which they were presented was counterbalanced across participants.

In the motor response localizer (**Fig. 1B, left panel**), participants responded to cues that explicitly indicated the required key presses. The cues were composed of four rectangles (200 by 100 pixels, approx. 4.8º by 2.4º) located along the horizontal axis of the screen, each indicating a response with a different finger: from left to right, with the left index, left middle, right index, or right middle finger. The cues were displayed against a black background, and to indicate the required response, the corresponding rectangle was filled in white. We employed these cues instead of verbal labels (as in the S-R mapping task) to avoid semantic processing during the localizer. Instead, we aimed to capitalize on the motor component, by generalizing across instructed response modalities (Liefooghe et al., 2012). Each trial of this localizer consisted of the presentation of the response cue for 1.5s, where participants responded, and a jitter ITI with a fixation cross (same temporal properties as above). Participants completed 80 trials, 20 for each response condition.

In the Action Effect localizer, we aimed to isolate the mappings' proximal action effects, i.e., the somatosensory consequences of the mapping responses (**Fig. 1B, middle panel**). To do so, we applied single-tap tactile stimulation on the tip of the participants' left and right

215 index and middle fingers, separately. To do so, we employed four MRI-compatible piezo-
216 electric stimulation devices (mini-PTS, http://www.dancerdesign.co.uk/), each covering an
217 area of 1cm^2 of the participants' fingertips. The stimulation pulses were generated with single
218 sawtooth waves, with 40ms of duration. We attached the stimulators to two foam structures,
219 one per hand, in an ergonomic position for the index and middle fingers. The intensity of the
220 stimulation was adjusted to the participants' sensitivity at the beginning of the MRI session.
221 In the localizer, the stimulation was applied while the cues from the motor response localizer
222 were displayed on the screen. Nonetheless, the cues were not informative about the
223 stimulated finger and all the rectangles appeared filled in black. This was done to keep the
224 two response-related localizers as similar as possible perceptually. Each trial consisted of
225 the pulse of stimulation (40ms) together with the presentation of the uninformative cues for
226 1.5s, both synchronized at the onset, and a jittered ITI (same temporal properties as above).
227 To facilitate the participants' engagement during the block, we added a secondary, memory
228 task in 16% of the trials. In these trials, the stimulation was not delivered, and the cues
229 appeared filled in color (pink, yellow, blue, or green). All participants saw the 4 colors in a
230 randomized order, with each color being shown in 4 trials. The participants were instructed
231 to pay attention and to remember the colors displayed, ignoring their appearance order.
232 When the localizer finished, the participants verbally reported the colors that they
233 remembered. The task consisted of 96 trials, and the stimulation was applied in 80 of them
234 (20 trials per stimulation condition).

235 Finally, participants completed a stimulus category localizer (**Fig. 1B, right panel**), where
236 they discriminated between animal and non-animal items. For each participant, we randomly
237 selected 80 animal pictures (20 per category) and 20 inanimate ones (10 musical
238 instruments, 10 vehicles) from the same database as in the S-R mapping task. All pictures
239 were 200 by 200 pixels, in greyscale, with the background removed and the item centered

on the image. In each trial, the stimulus was presented for 1.5s, followed by a jittered ITI (same temporal properties as above). Participants needed to respond simultaneously with their two index and middle fingers only when an inanimate stimulus appeared, which happened in 20% of the trials. In the remaining 80% of trials, an animal stimulus from one of four categories used in the mappings was shown, and no response was required. With this approach, we aimed to isolate the perceptual processing of the four animal categories, in the absence of any motor preparation or execution. The localizer consisted of 100 trials, 80 displaying an animal picture (20 per animal category).

All tasks were programmed in Psychopy (v3; Peirce et al., 2019) and were presented on a screen located at the back of the scanner and projected onto a mirror system. Responses were collected using a pair of MRI-compatible joysticks.

2.3. Experimental design

In the S-R mapping paradigm, we manipulated two within-subjects variables: the mappings' relevant responses ([left index, left middle], [left index, right index], [left index, right middle], [left middle, right index], [left middle, right middle], and [right index, right middle]), and stimulus category ([cat, dog], [cat, bird], [cat, fish], [dog, bird], [dog, fish], and [bird, fish]). We collected 48 trials per response and per category condition. For experimental control, we fully crossed these two variables, resulting in 36 different mappings pairs, sampled through eight observations each. However, all our analyses treated independently the response and category manipulations (e.g.: in the response-related analyses, we collapsed across stimulus categories within response conditions). Hence, our analyses were based on 48 observations per cell.

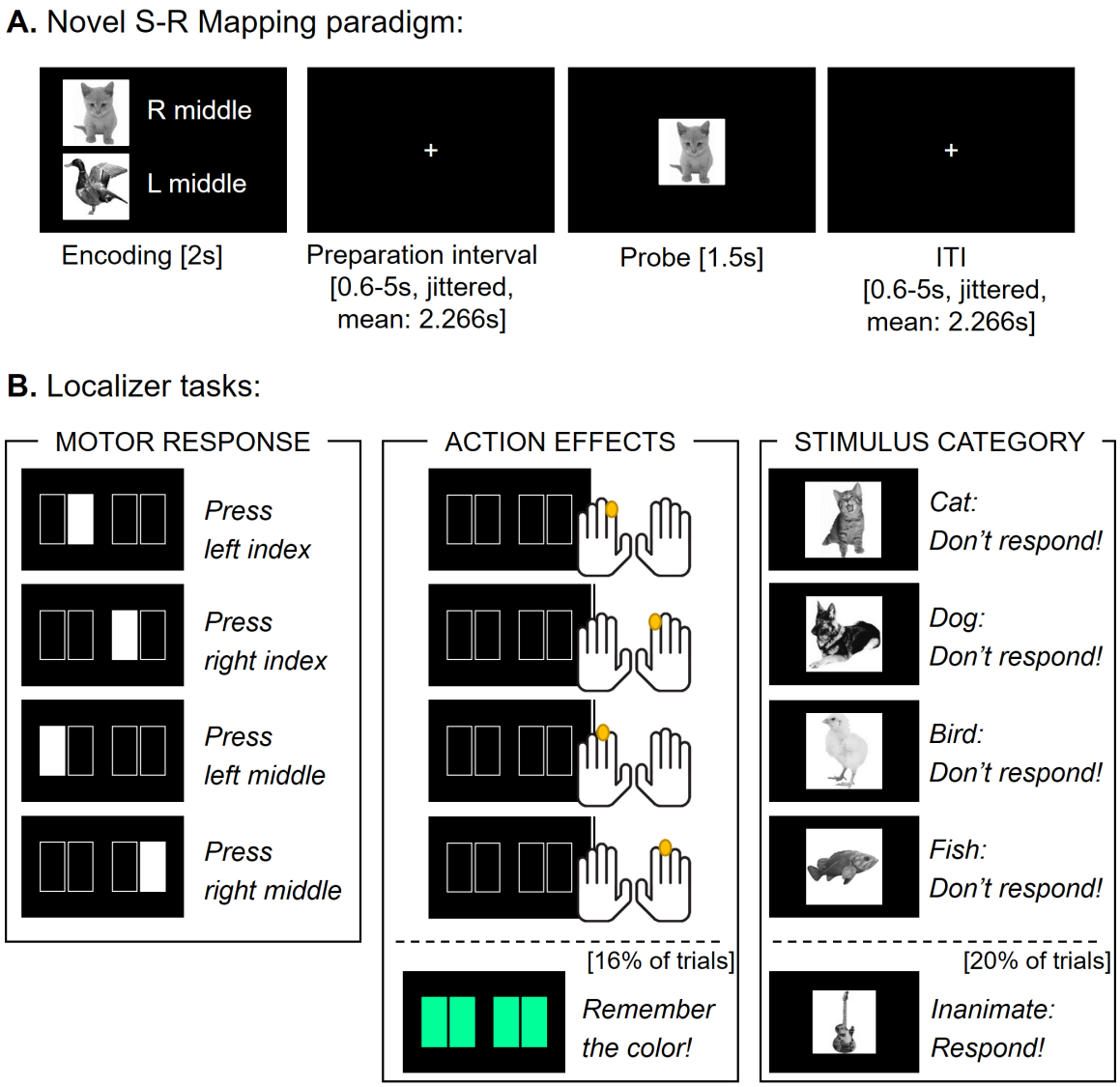

Figure 1. Experimental paradigms. **A.** Trial's sequence of events during the S-R mapping paradigm. **B.** Localizer tasks. In the motor response localizer (left panel), explicit cues indicated the required response (either with the left or right index or middle finger). In the action effect localizer (middle panel), stimulation was applied separately in each of these four fingers. The visual display consisted of uninformative cues, except for 16% of trials which entailed a secondary, color memory task. In the stimulus category localizer (right panel), pictures of animals belonging to the four categories used in the mappings were interspersed with pictures of inanimate items. Participants responded only to the infrequent (20%) inanimate stimuli.

In the motor response and action effects localizers, we had one within-subject manipulation: the effector (left index, left middle, right index, and right middle) used to respond or stimulate. In the stimulus category localizer, we manipulated within subjects the stimulus animacy (animate, and inanimate items) and the animal category of the animate stimulus (cat, dog, bird, and fish). In the three localizers, we collected 20 observations per condition of interest.

2.4. MRI data acquisition and preprocessing

The MRI data was collected with a 3T Siemens Magnetom Trio scanner at the Ghent University Hospital (UZ Ghent, Belgium) with a 64-channel head coil. Whole-brain functional images were obtained with a T2* EPI sequence [TR = 1730 ms, TE = 30 ms, flip angle=66°, FOV = 210 mm, image matrix = 84 × 84, voxel size = 2.5 x 2.5 x 2.5 mm, distance factor = 0%, 50 slices, slice acceleration factor = 2, slice orientation according to the participants' AC-PC line]. Four 400-volumes runs were collected for the S-R mapping task, and three 185-volumes runs for the localizers. Before the functional runs, we collected anatomical T1-weighted images using a MP-RAGE sequence [TR = 2250 ms, TE = 4.18 ms, flip angle=9°, FOV = 256 mm, image matrix = 256 x 256, voxel size = 1 x 1 x 1 mm, 176 slices]. We also collected phase and magnitude field map images [TR = 520 ms, TE1 = 4.92 ms, TE2 = 7.38 ms, flip angle=60°, FOV = 210 mm, image matrix = 70 × 70, voxel size = 3 × 3 × 2.5 mm, distance factor=0%, 50 slices], to correct for inhomogeneities of the magnetic field. Overall, participants remained inside the scanner for 75 minutes.

MRI Data preprocessing and GLM estimation (see section 2.6) were carried out on SPM12 (http://www.fil.ion.ucl.ac.uk/spm/software/spm12/). The functional images were spatially realigned, corrected for magnetic field inhomogeneities, and slice-time corrected. The T1 anatomical images were defaced, coregistered to the participants' mean functional volume, and segmented. For univariate analyses, the functional images were normalized to the MNI space using the forward deformation fields derived from the T1 segmentation and smoothed

296 with an 8mm FWHM Gaussian kernel. The multivariate analyses were performed on
297 unnormalized and unsmoothed images to avoid distorting the finer-grained activity patterns.
298 The normalization and smoothing were performed on the results maps. The T1
299 segmentation also generated inverse deformation fields which were used to convert the
300 ROIs masks, defined in the MNI space, into the participants' native anatomical space.

301 Four participants showed sustained, excessive movement (>2.5mm) and were removed
302 from the sample. However, 3 additional participants displayed punctual movements larger
303 than our voxel size but restricted on time. For those participants, the volumes affected by
304 movement (less than 1% of the acquired images) were masked in further analyses using
305 regressors generated with the ART toolbox (http://web.mit.edu/swg/software.htm).

306 2.5. Statistical analyses: behavioral data.

307 We analyzed the effect of the mappings' relevant responses and stimulus categories on
308 response accuracy and speed, separately. This was done in an exploratory fashion, to
309 assess whether the conditions were behaviorally balanced. We carried out repeated-
310 measures ANOVAs, using as within-subject factor either the response or the category
311 condition. A Greenhouse-Geisser correction was used when sphericity was violated. Post
312 hoc pair-wise *t*-tests were carried out to identify conditions where performance deviated from
313 the rest. A Bonferroni-Holm correction for multiple comparisons was applied. Catch trials
314 were excluded from the analyses. Only correct trials were included in RT ANOVAs.

315 2.6. Statistical analyses: fMRI data

316 *Univariate analyses*

317 We first conducted a series of univariate analyses to provide an overview of the regions
318 engaged by both the S-R mapping paradigm and the localizer tasks. For the S-R mapping
319 task, we fitted a GLM with regressors covering the mapping encoding stage, the preparation

interval, and the probe, separately for the six response conditions. Each regressor was defined using the event duration, except the probe, which was modeled with the trial RT. The ITI was not defined in the model and thus contributed to the implicit baseline. As nuisance regressors, we included errors, catch trials, and the six movement parameters derived from the realignment. Within participants, we carried out three one-sample *t*-tests to contrast each event of interest (encoding, preparation, and probe) against the baseline, collapsing across conditions. The outputs were entered into group-level *t*-tests to detect significant BOLD signal increases induced by our paradigm's events. The results were corrected at $p < .05$ using a cluster-wise FWE multiple-comparison correction (from an initial, uncorrected threshold of $p < .001$ and k = 10). For all the whole-brain analyses, the T values reported correspond to the cluster's peak.

The three localizers were analyzed in separate GLMs. For the motor response localizer, we defined a regressor for each response condition, locked to the onset of the response cue and with duration fixed to the trials' RT. Errors were included as a nuisance regressor. For the action effects localizer, the GLM included a regressor for each stimulation condition, locked and with the same duration as the stimulation pulse. Trials from the memory task were included as a nuisance regressor. Finally, for the stimulus category localizer, we modeled a regressor per animal category, with the same onset and duration as the stimulus presentation. Inanimate target trials and errors were included as nuisance regressors. The localizers GLMs also included the six motion parameters. We computed one-sample *t*-tests to detect BOLD signal increases linked to the localizers' event of interest (response, tactile stimulation, and target presentation) against the implicit baseline. We followed the same statistical inference strategy as with the S-R mapping task.

Canonical template tracking

The main goal of this study was to assess whether the motoric and visual representations guiding overt performance and perception were covertly engaged during novel mapping preparation. To do so, we employed a canonical template tracking procedure, a pattern analysis technique that enables the comparison of neural data between a targeted cognitive paradigm and theoretically driven localizer tasks (Palenciano et al., 2023; for other examples, see González-García et al., 2021; Wimber et al., 2015). Specifically, we estimated a series of canonical neural representations (or templates) from each localizer data. These templates aimed to capture the corresponding motoric or perceptual component representation in the same format as engaged during overt processing (i.e., pressing a key, experiencing the action effect, or perceiving the stimulus category). Then, we assess the representational strength of these templates during the S-R mapping paradigm, by computing their similarity with the multivoxel activity patterns evoked by the novel mappings' preparation interval.

First, we fitted a set of GLMs to estimate the multi-voxel activity patterns during the S-R mapping task (**Fig. 2A**). To maximize the number of data points being fed into the template tracking procedure, we estimated the signal in a trial-by-trial fashion. We used a least-square-sum (LSS) approach (Arco et al., 2018; Mumford et al., 2012, 2014) to reduce the collinearity. For each trial, we estimated a separate GLM with the following regressors: (1) the preparation interval of the current trial; (2) the encoding stage, collapsing across all correct trials; (3) the preparation stage, excluding the current trial but collapsing across the remaining correct trials; (4) the probe event, collapsing across all correct trials. All trial-wise GLMs further included nuisance regressors modelling, (5) errors and (6) catch trials (using the same onset and duration as in the univariate GLM defined above), and the six movement parameters. We iterated the estimation procedure across all the trials, obtaining a beta map

368 for the preparation interval of each pair of novel mappings. Next, we performed one-sample
369 *t*-tests comparing each beta map against the baseline, to normalize noise from a univariate
370 perspective (Kriegeskorte et al., 2008; Walther et al., 2016). The activity patterns used for
371 the template tracking were directly extracted from the resulting trial-wise *t*-maps.

372 Next, we estimated the canonical neural templates using the three localizers' data (**Fig. 2B**).
373 To maximize the robustness of the templates, we estimated standard GLMs that provided a
374 single beta map per localizer condition. Within each localizer, the four conditions' beta
375 images (corresponding to the four effectors in the case of the motor response and action
376 effects localizers, and to the four animal categories in the stimulus category localizer) were
377 contrasted separately against the baseline. The templates were extracted from the resulting
378 *t*-maps.

379 Finally, we estimated the similarity between the templates and each activity pattern from the
380 mappings' preparation interval (**Fig. 2C**). In each trial from the S-R mapping task, two out of
381 the four possible motor responses, and two out of the four possible stimulus categories,
382 were prepared in advance. This design allowed distinguishing between two subsets of
383 templates regarding a given trial: relevant (i.e., prepared) and irrelevant (i.e., not prepared)
384 ones. Hence, we estimated the similarity between the main task data and both types of
385 templates and used the irrelevant similarity measurements as baseline. Critically, the use of
386 this baseline condition allowed us to infer the specificity of the motoric and perceptual
387 information encoded during the preparation (Palenciano et al., 2022). To compare the
388 similarity estimates from several templates simultaneously, while accounting for the shared
389 variance among them, we used a multiple regression framework (e.g., Palenciano et al.,
390 2019).

391 We first carried out the template tracking separately for each localizer task and on a set of
392 ROIs (see *ROI selection* section). For each region, we first normalized (i.e., z-scored) each

activity pattern from the S-R mapping task and each canonical template, ensuring that all of them had a mean of 0 and a standard deviation of 1. That sought to mitigate the impact of univariate activity differences on our canonical template results. Then, we fitted a series of multiple regressions in which the multi-voxel activity pattern from a trial's preparation interval was predicted using the four localizer templates as regressors. That provided beta coefficients that reflected the similarity between relevant and irrelevant templates and the main task data. Then, we averaged the beta weights across templates and trials to obtain a single relevant and irrelevant value per ROI. At the group level, we carried out one-tailed, paired-sample Wilcoxon signed rank tests to assess the hypothesis that the beta weights from relevant templates were higher than the irrelevant ones. This comparison offered an estimate of the representational strength of specific templates while controlling for more general motor preparation or visual expectation processes. Furthermore, one-sample Wilcoxon tests were performed to assess whether relevant and irrelevant beta weights were different from zero. It is important to note that the later results could be contaminated by the positive bias present in similarity estimates, and hence, were only interpreted to qualify the comparison against the irrelevant (or baseline) condition. In all cases, we controlled for multiple comparisons (i.e., number of ROIs) using a Bonferroni-Holm correction (Holm, 1979).

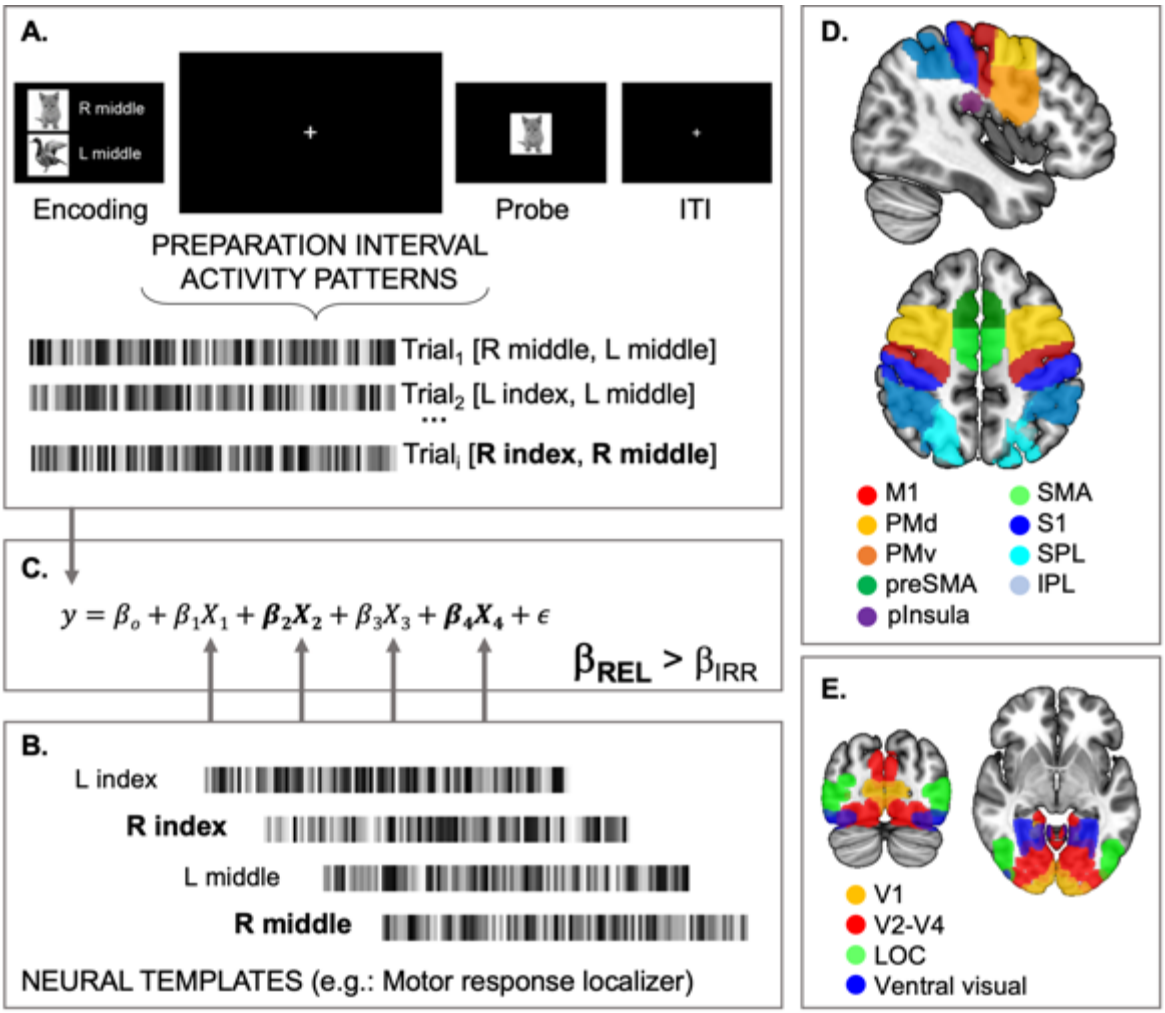

Figure 2. Canonical template tracking. **A.** Estimation of trial-by-trial activity patterns from the preparation interval of the S-R mapping paradigm. In the trial shown as an example ($Trial_i$), the prepared mapping responses entailed the right index and middle fingers. **B.** Canonical template estimation. From each localizer, we estimated a single activity pattern per condition. Here we illustrate the motor response localizer, with templates corresponding to the four response conditions. The templates relevant to the mapping are shown in bold. **C.** A multiple regression was fitted to predict each trial's activity pattern. The regressors entailed the four (two relevant, in bold, and two irrelevant) canonical templates, together with a constant and an error term. The inference was carried out on the comparison between averaged beta weights from relevant and irrelevant templates. **D.** ROIs used in the motor response and action effect analyses. **E.** ROIs used in the stimulus category analyses.

422 Since the motor response and the action effects localizers tapped into a common component
423 of the S-R mappings, we performed an additional analysis including templates from the two
424 localizers simultaneously. With this approach, we aimed to disentangle the contribution of
425 passive perception of the action effects, from a richer action representation conveying motor
426 planning and execution. The procedure was identical to the one specified above, with the
427 exception that the multiple regressions included eight regressors (one per effector condition
428 and localizer) instead of four. After averaging, we obtained four estimates per ROI,
429 corresponding to relevant and irrelevant motor response and action effects templates. Next,
430 we carried out a repeated measures ANOVA including the ROI, the localizer task, and the
431 template condition (relevant, irrelevant) as within-subject factors. We carried out post hoc
432 comparisons to explore the three-way interaction between ROI, Localizer, and Template,
433 using a Bonferroni-Holm multiple comparison correction.

434 *Response templates: exploratory analyses*

435 In addition to our planned analyses, we aimed to better understand which aspects of the
436 mappings' instructed responses were captured by our canonical templates. In this regard,
437 the novel mappings involved different response effectors (index, middle fingers) and
438 different laterality (left-hand, right-hand responses). Due to the pervasive effects of response
439 laterality, we aimed to address whether specific response effector representations could be
440 also detected with the canonical template procedure. While the experiment was designed to
441 control for laterality, by balancing it across the response conditions, we further investigated
442 this issue by repeating our main analysis in a subset of novel mappings where only the
443 templates' effector information (and not the laterality) was relevant. First, we extracted the
444 relevant and irrelevant beta weights from S-R mappings that entailed the same effector from
445 the two hands (i.e., the conditions [left index, right index] and [left middle, right middle]) and
446 estimated the activation of the relevant effector templates in comparison with the irrelevant

ones. In each of the targeted conditions, the relevant and irrelevant templates would differ only regarding the response effector being equated regarding response laterality. We carried out this comparison in all the ROIs examined in the main analysis. Second, to provide a deeper insight into the processes implemented in the primary motor and somatosensory cortex, we carried out an additional test on these ROIs using the same subset of trials but further differentiating the laterality of the templates. Specifically, each canonical template was estimated using data from the contralateral hemisphere ROIs. For instance, to predict the activity patterns of mappings involving [left index, right index], we used data from the left M1 to estimate the similarity with the right index (relevant) and right middle (irrelevant) templates, and data from the right M1 to estimate the similarity with the left index (relevant) and left middle (irrelevant) templates. This way, we ensured that our results were driven by specific effector representations engaged in the corresponding, contralateral primary cortex. Nonetheless, it is important to stress the post hoc nature of these analyses, for which the experiment design was not optimized. As a result, only 33% of the observations from the S-R mapping task were included, with a corresponding negative impact on the analysis's statistical power. Still, these results helped qualify the planned analyses here reported.

Finally, we aimed to ensure that our main findings were not driven by motoric brain signals that spread from the probe epoch into the preparation interval. Considering the temporal proximity of these two events and the sluggishness of the fMRI BOLD signal, it could be argued that signals originated during task execution could contaminate the preparatory activity patterns. To prevent this confound, we employed a validated jittered distribution (e.g., González-García et al., 2021) and used an LSS estimation protocol that facilitated signal segregation (Arco et al., 2018; Mumford et al., 2012, 2014). Still, we performed a series of further tests to evidence that template instantiation could be detected in the absence of later action. In our task, only one of the two S-R mappings – and thus, prepared

472 responses –were actually executed after the preparation interval. Hence, we focused on the
473 prepared but not executed mappings and repeated the above-described response-related
474 canonical template analyses. Specifically, we replicated the ROI-based multiple regression
475 (using the motor response and action effects templates both independently and
476 simultaneously) including a single relevant template: the one corresponding to the prepared
477 response that was not executed in the current trial. Replicating the same pattern of results
478 in these analyses would strongly argue against signal misattribution.

479 *ROI selection*

480 We used two sets of a-priori ROIs, one for the motor response and action effects templates,
481 and another one for the stimulus category ones. In the former case, we selected regions
482 associated with action control and somatosensory processing. Specifically, we focused on
483 the primary motor (M1) and somatosensory cortex (S1), the ventral and dorsal portion of the
484 premotor cortex (PMv and PMd, respectively), the supplementary and pre-supplementary
485 motor areas (SMA and preSMA, respectively), and the inferior and superior parietal lobe
486 (IPL and SPL, respectively). A post hoc ROI was placed on the posterior insula (pInsula)
487 due to its involvement during the tactile stimulation processing (see **Fig. 4**). The impact of
488 the stimulus category templates was assessed in regions processing both physical stimulus
489 attributes and more abstract, categorical information. Specifically, we used as ROI the
490 primary visual cortex (V1), the early visual cortices from V2 to V4 (V2-V4), the lateral
491 occipital complex (LOC), and a broader region covering the ventral pathway until the
492 inferotemporal cortex (VentralVisual).

493 The M1, PMv, PMd, SMA, preSMA, and S1 ROIs were obtained from the Human Motor Area
494 Template (HMAT; Mayka et al., 2006), while the IPL, SPL, V1, V2-V4, LOC, and
495 VentralVisual masks were extracted from the HCP-MMP1.0 parcellation (Glasser et al.,
496 2016). All ROIs covered the bilateral portions of the corresponding region, except for the M1

497 and S1, for which we used separated ROIs for the left and right hemispheres to account for
498 their contralateral functional organization. This was done to avoid capturing broader
499 interhemispheric differences in univariate signal that would remain after the z-score
500 correction. Finally, we used MarsBar (http://www.sourceforge.net/projects/marsbar) for the
501 pInsula, building two 10mm radius spherical ROIs located in the bilateral activation peaks
502 found in the univariate results from the action effect localizer.

503 For each localizer, we included a control ROI that was unrelated to the templates of interest
504 and where no effects were expected. Specifically, we used V1 in the motor response and
505 action effects analyses, and M1 in the stimulus-related analysis.

506 *Whole-brain searchlight analyses*

507 To complement the ROI results, we additionally performed exploratory whole-brain analyses
508 using a searchlight procedure. We iterated a 5-voxel radius sphere across every location of
509 the brain, performing multiple regressions with the S-R mapping task activity patterns and
510 templates estimated from the current sphere data. The averaged beta coefficients for the
511 relevant and irrelevant templates were assigned to the voxel at the center of the sphere. As
512 a result, we obtained two beta maps per participant and localizer task, one for the relevant
513 and another for the irrelevant templates. Next, within participants, we subtracted the
514 irrelevant beta map from the relevant one. The resulting images were normalized and
515 smoothed, and entered into group-level one-sided, one-sample *t*-tests to detect significantly
516 greater beta weights linked to relevant templates, in comparison with irrelevant ones.

517 We further used the searchlight whole-brain maps to formally test whether univariate and
518 multivariate preparatory signals overlapped anatomically. To do so, we thresholded ($p < .05$,
519 FEW corrected) and binarized the group-level brain maps obtained in the univariate *t*-test
520 from the preparation interval and the three canonical template tracking searchlights. Then,

521 we computed the conjunction between each pair of univariate and multivariate maps to
522 identify the voxels that remained significant in the two contrasts (Nichols et al., 2005).

523 *Control analysis: template reliability.*

524 Finally, we aimed to ensure that our results were not driven by differences in the reliability
525 of the canonical templates employed. The experimental design sought to eliminate such
526 confound by balancing each localizer's set of templates (e.g., the four response effectors'
527 templates) between the relevant and irrelevant conditions. Nonetheless, we computed two
528 reliability measurements per template (González-García et al., 2021; Palenciano et al.,
529 2023). First, to estimate the overall univariate noise, we computed the Signal-to-Noise Ratio
530 (SNR), dividing the absolute mean t value from a given template by its standard deviation.
531 Then, to assess the stability of the templates' informational content, we used a
532 correlationability index (González-García et al., 2021). We split each localizer data into odd
533 and even trials and fitted new GLMs, obtaining two (instead of a single) canonical templates
534 per localizer condition. The correlationability index consisted of the Pearson correlation
535 coefficient between each condition's pair of templates. To identify reliability differences
536 among templates, we run one-way repeated measures ANOVAs separately for each
537 measurement, localizer, and ROI. The template condition was used as a single factor. Post
538 hoc paired-sample *t*-tests (Bonferroni-corrected for multiple comparisons) were computed
539 whenever the main effect of the template condition was significant.

540 **3. Results**

541 3.1. Behavioral results.

542 Performance was in line with previous studies using novel S-R associations. On average,
543 participants responded accurately on 89% of trials of the S-R mapping task (SD = 6%), with
544 a mean RT of 710 ms (SD = 99 ms). On catch trials, the average accuracy was 84% (SD =

22%), and the mean RT, 943 ms (SD = 134 ms). Regarding the localizers' performance, in the motor response task, participants responded correctly in 98% of trials (SD = 1.7%), with an average RT of 523 ms (SD = 58 ms). In the action effects localizer, all the participants recalled correctly the four colors used in the secondary memory task. Finally, in the stimulus category localizer, the mean accuracy was 99% (SD = 12%), with an average of 0.2% of false alarms (SD = 0.5%) and 4% of misses (SD = 8%). The average RT was 942 ms (SD = 14 ms).

We explored whether the behavioral performance was modulated by the mappings' relevant responses and stimulus categories. The response condition effect (**Fig. 3**) was not significant neither accuracy rates, $F(3.4, 99.9) = 0.83$, $p = .49$, $\eta_p^2 < .01$, nor in RTs, $F(5, 145) = 1.36$, $p = .24$, $\eta_p^2 = .05$, supporting that performance was equivalent across response pairings. Regarding the stimulus category (**Fig. 3**), however, we found a significant effect on both accuracy rates, $F(5, 145) = 3.84$, $p = .003$, $\eta_p^2 = .12$, and RTs, $F(5, 145) = 2.38$, $p = .04$, $\eta_p^2 = .08$. Post hoc paired-sample *t*-test showed that, in general, participants performed worst mappings that included the category pair [bird-fish]. Accuracy was lower in this condition than in the [cat-dog] pair ($T = 3.43$, $p = .01$) and the [cat-fish] pair ($T = 3.90$, $p = .002$), with an additional marginal difference with the [cat-bird] pair ($T = 2.84$, $p = 0.07$). RTs were marginally slower in [bird-fish] trials than in [dog-fish] ones ($T = 2.79$, $p = 0.09$). More qualitatively, the overall pattern reflected a general impoverishment in the [bird-fish] category pairings than in the other conditions.

Finally, to explore whether the S-R mappings combination further modulated behavioral performance we carried out additional repeated measures ANOVA including the response and the category condition as factors. In line with the above-described results, the effect of category was significant for both RT, $F(4.31, 124.84) = 2.54$, $p = .03$, $\eta_p^2 = .08$, and accuracy

rates, F(4.22, 122.23) = 3.84, p = .003, η_p^2 = .12. Contrary, neither the response condition nor the interaction was significant (all *p values* > .20).

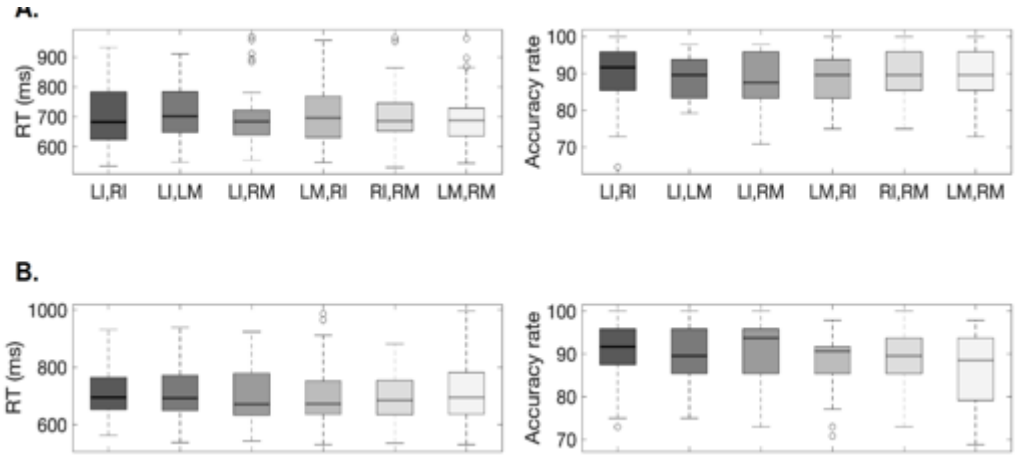

Figure 3. Boxplots displaying the RTs (left) and percentage of correct responses (right) during the novel S-R Mapping paradigm across the six response conditions **(A)** and six stimulus category conditions **(B)**. LI = left index; RI = right index; LM = left middle; RM = right middle.

3.2. fMRI results

Univariate analyses

As a first step, we aimed to characterize the regions engaged by the different stages of the S-R mapping paradigm. Replicating previous findings, encoding novel S-R associations was associated with increased activity broadly in the MDN and the visual and motor systems (**Fig. 4A**). A wide cluster ([38, -66, -16], k = 57033, T(1,29) = 20.05, p < .001) covered the early and late visual cortices, extending dorso-medially into the precuneus and anteriorly into the inferotemporal cortex. The cluster also included S1, M1, PMC, and SMA. Within the MDN, it covered the lateral DLPFC, incurring into the anterior insula/frontal operculum (aI/fO) in the left hemisphere, and the SPL, IPL, and IPS. It also covered part of the cerebellum and the thalamus. A second cluster ([32, 22, 4], k = 539, T(1,29) = 7.50, p < .001) covered the right aI/fO. Conversely, during the mappings' preparation interval (**Fig. 4B**), only a restricted set of regions showed a consistent activity increase. Specifically, we

588 found significant clusters bilaterally in the aI/fO (left: [-30, 20, -2], k = 867, T(1,29) = 13.49,
589 $p < .001$; right: [34, 22, -2], k = 825, T(1,29) = 14.38, $p < .001$), the inferior frontal junction
590 (left: [-42, 24, 28], k = 258, T(1,29) = 5.58, $p = .001$); right: [40, 30, 30], k = 442, T(1,29) =
591 7.28, $p < .001$), the preSMA ([6, 20, 50], k = 1323, T(1,29) = 11.61, $p < .001$), and the bilateral
592 IPS and IPL (left: [-32, -54, 42], k = 376, T(1,29) = 6.60, $p < .001$; right: [36, -54, 42], k =
593 387, T(1,29) = 7.15, $p < .001$). Finally, probe processing (**Fig. 4C**) substantially engaged the
594 visual and motor system and the MDN, as well as subcortical nuclei. An extended cluster
595 ([36, 2, 10], k = 104250, T(1,29) = 19.61, $p < .001$) overlapped with the activations found
596 during the encoding, also including the premotor cortices, the preSMA, the middle cingulum,
597 the middle and posterior region of the insula, the temporal operculum, the rostrolateral
598 prefrontal cortex, and the basal ganglia.

599 With a similar approach, we described the regions engaged by the three localizers' events
600 of interest (**Fig. 4D**). As expected, the motor response localizer induced an increase in
601 activity in regions associated with action control. A wide cluster ([20, -88, -12], k = 32523,
602 T(1,29) = 10.60, $p < .001$) bilaterally covered the motor cortices, including M1, premotor
603 cortices, and SMA, and extended into the S1, SPL, and IPL. As expected from the presence
604 of visual stimulation during this localizer, the cluster also included early and late visual
605 cortices. Two additional clusters were found in the basal ganglia and posterior insula in both
606 hemispheres (left: [-46, 0, 12], k = 2418, T(1,29) = 8.45, $p < .001$; right [28, 0, 2], k = 1223,
607 T(1,29) = 7.14, $p < .001$). Conversely, the tactile stimulation applied in the action effect
608 localizer was linked to increased activity in the pInsula, bilaterally (left: [-46, -20, 14, k = 950,
609 T(1,29) = 8.63, $p < .001$; right: [50, -24, 22], k = 1046, T(1,29) = 7.29, $p < .001$). This task
610 also recruited the early visual cortex ([24, -90, 4], k = 4269, T(1,29) = 13.65, $p < .001$), .
611 Finally, the stimulus category localizer was associated with heightened activity in a cluster
612 covering the bilateral early and late visual cortex and the right SPL and IPL (left: [-38, -84, -

2], k = 7009, T(1,29) = 14.43, $p < .001$; right: [40, -82, -4], k = 8761, T(1,29) = 15.52, $p < .001$), and another cluster located in the left SPL and IPL ([-22, -48, 40], k = 575, T(1,29) =6.54, $p < .001$). Increased activity was also found in the bilateral hippocampus (left: [-22, 30, 0], k = 224, T(1,29) = 7.26, $p < .001$; right: [22, -30, -2], k = 273, T(1,29) = 7.41, $p < .001$).

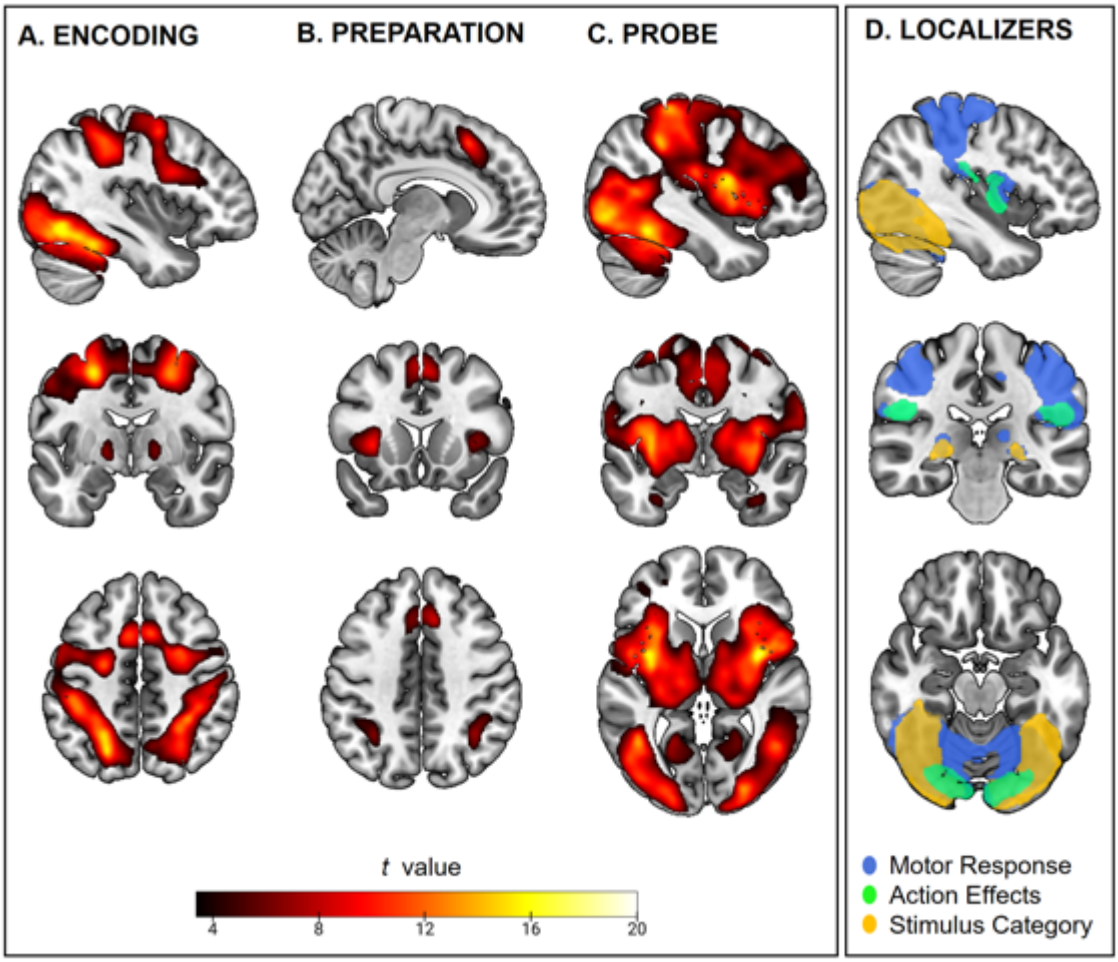

Figure 4. Univariate analysis results. **A.** *t* maps showing the increases in activity associated with the encoding (left panel), preparation (middle panel), and implementation (right panel) of the novel S-R mappings. **B.** *t* maps showing the increases in activity associated with the three localizers' event of interest: the response in the motor response localizer (in blue), the tactile stimulation in the action effects localizer (in green), and the animate picture visualization in the stimulus category localizer (yellow). All maps are statistically thresholded at $p < .05$. The unthresholded whole-brain maps used to generate this figure are available in NeuroVault: https://neurovault.org/collections/XQFLCDUH/

Canonical template tracking: ROI analyses

To address the main goal of this work, we conducted a series of multivariate, ROI-based analyses which informed on whether the preparation to implement novel S-R mappings activated templates of the instructed responses and stimuli. On one hand, we explored how the novel mappings' responses were represented, using templates estimated from the motor response and the action effects localizers. On the other, we also addressed the anticipatory encoding of the mappings' stimuli, using templates from the stimulus category localizer.

Response-related analyses

The results obtained using the motor response templates are displayed in **Fig. 5A** and **Fig. 5-1**. First, we assessed whether the relevant motor response templates were activated to a greater degree than the irrelevant ones, using the latter as baseline. The results supported this hypothesis in most of the regions explored. The paired-sample Wilcoxon tests were significant in the left and right M1 and S1, SMA, PMd, IPL, SPL, and pInsula. Additional one-sample tests showed that the relevant templates' beta coefficients were greater than zero in all these regions and the PMv. Finally, after visually inspecting our data, we observed that some regions' irrelevant templates were linked to below-zero beta coefficients. The corresponding one-sample tests on irrelevant template data evidenced significant below-zero beta weights in the left and right M1 and S1, and the pInsula. Contrary, significant above-zero irrelevant templates' beta weights were found in the PMv. As expected, neither test was significant in the control ROI, V1.

Next, we applied the same analytical approach with the templates obtained from the action effects localizer (**Fig. 5B**, **Fig. 5-1**). Like the motor response, the beta weights from relevant and irrelevant action effect templates differed in most of the ROIs. The effect was significant in the right M1, the left and right S1, the SMA, PMd, IPL, SPL, and pInsula. The relevant templates were linked to statistically significant above-zero beta weights across all these

650 regions and the left M1. Finally, we found below-zero beta coefficients linked to irrelevant
651 action effects templates in the left S1 and pInsula. Again, neither test was significant in V1.

652 Considering the equivalent pattern of results obtained with the two response-related
653 localizers and the nature of both tasks, our findings could also reflect that the motor response
654 and action effects templates captured overlapping representations, and consequently,
655 shared variance from the mappings' activity patterns. To estimate the unique variance
656 explained by each localizer, we ran an additional analysis including the templates from both
657 tasks simultaneously in the multiple regressions. The resulting averaged beta coefficients
658 are displayed in **Fig. 5C and Fig. 5-2.** To explore these results, we ran repeated measures
659 ANOVA on the beta weights, using ROI (left M1, right M1, left S1, right S1, SMA, preSMA,
660 PMv, PMd, IPL, SPL pInsula), Localizer (motor response, action effects), and Template
661 (relevant, irrelevant) as factors. We found significant main effects of Template, $F(1, 26) =$
662 216.65, $p < .001$, $\eta^2_p = .893$, and ROI, $F(5.80, 150{,}80) = 2.76$, $p = .015$, $\eta^2_p = .096$, but not
663 of Localizer, $F(1, 26) = 0.25$, $p = .619$, $\eta^2_p = .010$. Nonetheless, the interaction between
664 Localizer and Template was significant, $F(1, 26) = 19.60$, $p < .001$, $\eta^2_p = .430$, supporting
665 that the localizer task modulated the relationship between relevant and irrelevant templates.
666 To address the anatomical extent of this effect, we next focused on the significant three-way
667 Localizer x Template x ROI interaction, $F(4.89, 127.07) = 18.20$, $p < .001$, $\eta^2_p = .412$, and
668 ran post hoc comparisons contrasting relevant and irrelevant templates separately for each
669 localizer and ROI (**Table 2**). These tests showed a generalized increase in beta coefficients
670 in relevant than irrelevant templates in the two localizer tasks. Significant differences
671 involving motor response and action effect templates were found in left and right M1 and
672 S1, SMA, PMd, IPL, SP, and pInsula. The test was also significant for the action effect
673 templates in the preSMA. Overall, even when the templates' effect was numerically different
674 depending on the localizer (as evidenced by the two-way and three-way significant

interactions), it persisted after including the two localizers' data simultaneously in the analysis, suggesting that both sets of templates captured independent aspects of the S-R mapping task data.

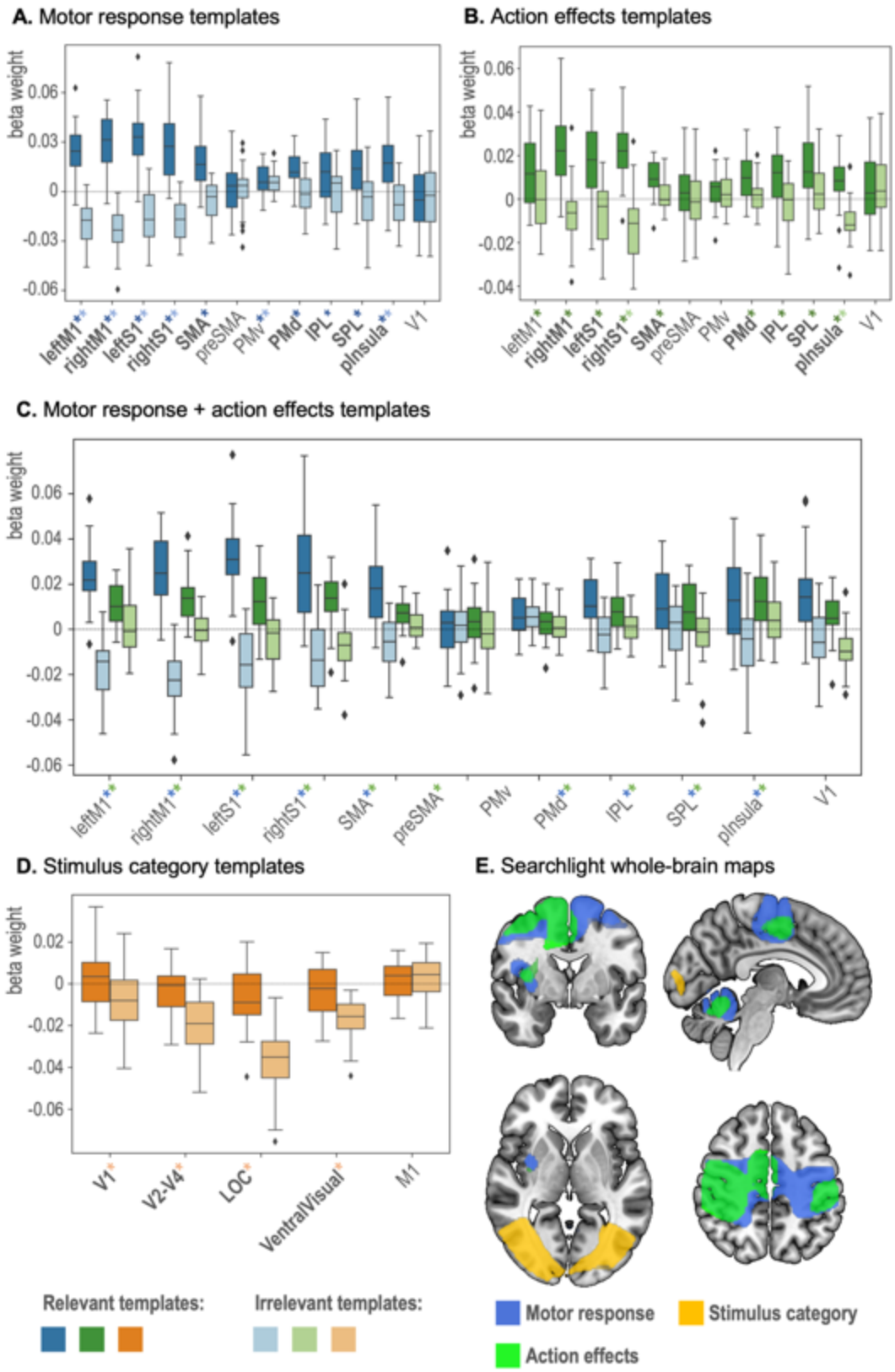
A. Motor response templates
B. Action effects templates
C. Motor response + action effects templates
D. Stimulus category templates
E. Searchlight whole-brain maps
beta weight
leftM1
rightM1
leftS1
rightS1
SMA
preSMA
PMv
PMd
IPL
SPL
pInsula
V1
V2-V4
LOC
VentralVisual
M1
Relevant templates:
Irrelevant templates:
Motor response
Stimulus category
Action effects

678

Figure 5. Canonical template tracking results. **A-D:** Boxplots displaying the beta weights for relevant and irrelevant canonical templates. **A.** Motor response localizer results. **B.** Action effects localizer results. **C.** Results after including the motor response and the action effect templates in the same multiple regressions. **D.** Stimulus category localizer results. In **A**, **B**, and **D**, bold ROI labels indicate that the relevant beta weights are significantly greater than the irrelevant ones, and the asterisks, that either the relevant or the irrelevant beta weights (shown in the corresponding darker or lighter color shade) are significantly different than zero. In **C,** the asterisks indicate that, for a given localizer (indicated by the asterisk color, blue: motor response, green: action effects), the relevant beta weights are significantly greater than the irrelevant ones. **E.** Searchlight whole-brain maps, showing clusters with significantly higher beta weights from relevant than irrelevant templates. The unthresholded whole-brain maps used to generate this figure are available in NeuroVault: https://neurovault.org/collections/XQFLCDUH/

Response templates: exploratory analyses

In addition to our planned analyses, we further explored the response attributes that the motor response and action effects templates were capturing. The visual inspection of the motor response (**Fig. 5-4**) and action effect (**Fig. 5-5**) beta weights across the six response conditions highlighted the robust effect of response laterality, especially, in primary and secondary somatomotor areas. That could be identified in trials where the division between relevant and irrelevant templates was mapped into different laterality (i.e., in the mappings' response conditions [left index, left middle] and [right index, right middle]). To rule out that our results were uniquely driven by differences between right- and left-hand response representations, we first compared relevant and irrelevant templates in a subset of trials in which only the effector information was relevant for the analysis. The results from the motor response localizer (**Fig. 6A**) showed greater beta weights for relevant than irrelevant templates in the right S1 (z = 2.76, p = .002, $p_{corrected}$ = .032). A similar pattern was found in the right M1 (z = 2.24, p = .013, $p_{corrected}$ = .124) and the SPL (z = 1.71, p = .044, $p_{corrected}$ =

.394), although these tests did not survive the correction for multiple comparisons. Regarding the action effects templates (**Fig. 6B**), we found a significant effect in the left S1 (z = 2.80, p = .003, $p_{corrected}$ = .028). Next, we aimed to shed some light on the representations instantiated in M1 and S1. Since these two regions have clear contralateral neural architecture, we analyzed separately the two hemispheres' data. Specifically, we used data from the contralateral hemisphere of specific mappings and templates to perform the analysis. The tests contrasting relevant and irrelevant templates remained significant in S1 when using data from either the motor response (**Fig. 6C**) or the action effect localizers (**Fig. 6D)**. Specifically, we found a significant effect of the motor response templates in the right S1 (z = 2.67, p = .004, $p_{corrected}$ = .016), and the action effects templates in the left S1 (z = 2.97, p = .002, $p_{corrected}$ = .002). An equivalent pattern was found in the left and right M1, although neither test survived the statistical correction (Motor response, right M1: z = 1.60, p = .054, $p_{corrected}$ = .188; Action effects, left M1: z = 1.50, p = .066, $p_{corrected}$ = .081).

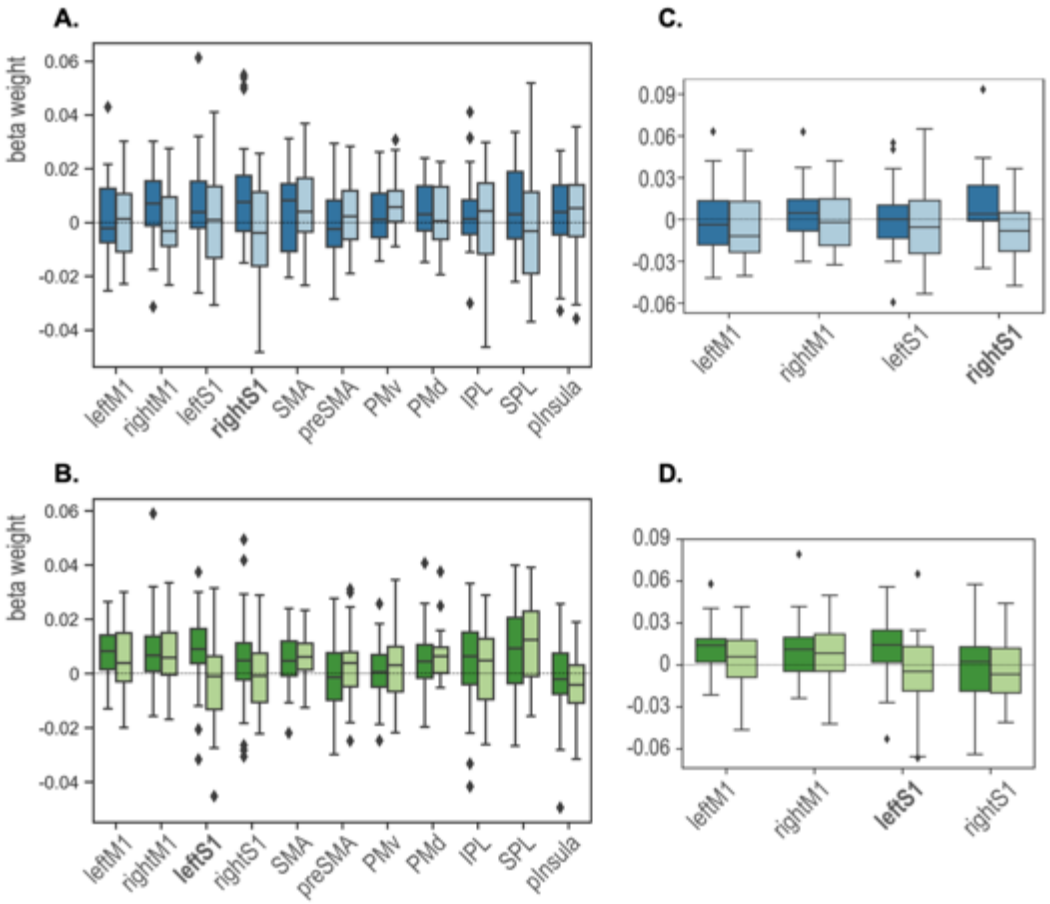

Figure 6. Boxplots showing the beta weights for relevant and irrelevant templates capturing the mappings' response effector information. **A,B.** Results from the [Left Index, Right Index] and [Left Middle, Right Middle] trials, using the motor response (**A**) and action effects (**B**) templates. **C,D.** Results using activity patterns from the M1 and S1 ROIs contralateral to the mappings' and canonical templates' laterality condition, using data from the motor response (**C**) and action effects (**D**) localizer. The ROI labels shown in bold indicate that the relevant beta weights are significantly greater than the irrelevant ones after controlling for multiple comparisons.

Finally, we carried out a series of analyses restricted to the mapping responses that were prepared but not implemented, to ensure that our main results were not driven by motoric signals spreading from the task execution epoch. We repeated the ROI-based canonical template procedure including, in the multiple regression, a single relevant template corresponding to the non-executed mapping response. In general terms, these results

replicated most of the reported effects. Using the motor response templates, the paired-sample tests comparing relevant irrelevant templates were significant in left M1 (z = 4.38, p < .001, $p_{corrected}$ < .001), right M1 (z = 4.75, p < .001, $p_{corrected}$ < .001), left S1 (z = 4.22, p < .001, $p_{corrected}$ < .001), right S1 (z = 4.53, p < .001, $p_{corrected}$ < .001), SMA (z = 4.05, p < .001, $p_{corrected}$ < .001), PMd (z = 3.13, p < .001, $p_{corrected}$ = .002), SPL (z = 2.37, p = .009, $p_{corrected}$ < .020) and pInsula (z = 3.50, p < .001, $p_{corrected}$ < .001). The relevant template beta weights, associated with the prepared but not executed response, were statistically greater than zero in left M1 (z = 3.71, p < .001, $p_{corrected}$ < .001), right M1 (z = 3.71, p < .001, $p_{corrected}$ < .001), left S1 (z = 4.29, p < .001, $p_{corrected}$ < .001), right S1 (z = 4.10, p < .001, $p_{corrected}$ < .001) SMA (z = 3.51, p < .001, $p_{corrected}$ < .001), PMv (z = 3.34, p < .001, $p_{corrected}$ = .003), PMd (z = 3.81, p < .001, $p_{corrected}$ < .001), SPL (z = 2.44, p = .015, $p_{corrected}$ = .031) and pInsula (z = 2.91, p = .003, $p_{corrected}$ = .009). The irrelevant templates were associated with statistically significant below-zero beta weights only in the left M1 (z = -3.01, p = .003, $p_{corrected}$ = .014).

Equivalent tests performed with the action effects templates showed greater relevant than irrelevant beta weights in right M1 (z = 3.28, p < .001, $p_{corrected}$ = .004), left S1 (z = 3.30, p < .001, $p_{corrected}$ = .004), right S1 (z = 3.54, p < .001, $p_{corrected}$ < .001), PMd (z = 2.46, p = .007, $p_{corrected}$ = .034) and pInsula (z = 3.26, p < .001, $p_{corrected}$ = .007). The relevant template beta weights were greater than zero in left M1 (z = 2.93, p = .003, $p_{corrected}$ = .011). right M1 (z = 3.77, p < .001, $p_{corrected}$ < .001), left S1 (z = 3.03, p = .002, $p_{corrected}$ = .008), right S1 (z = 3.53, p < .001, $p_{corrected}$ < .001), SMA (z = 3.24, p = .001, $p_{corrected}$ = .004), PMd (z = 3.48, p < .001, $p_{corrected}$ = .001), and SPL (z = 2.98, p = .002, $p_{corrected}$ = .011). Conversely, no significant below-zero beta coefficients were found for the irrelevant templates in this analysis.

Finally, when the motor response and action effect templates were simultaneously included in the multiple regression, significant differences between relevant and irrelevant beta were found for both localizers in left S1 (motor response: z = 3.98, p < .001, $p_{corrected}$ < .001; action

effects: z = 3.11, p < .001, $p_{corrected}$ = .013), right S1 (motor response: z = 4.24, p < .001, $p_{corrected}$ < .001; action effects: z = 2.90, p = .002, $p_{corrected}$ = .019) and pInsula (motor response: z = 2.85, p = .002, $p_{corrected}$ = .014; action effects: z = 3.06, p = .001, $p_{corrected}$ = .026). A similar result, although marginally significant for the action effects' templates, was found in right M1 (motor response: z = 4.48, p < .001, $p_{corrected}$ < .001; action effects: z = 2.46, p = .006, $p_{corrected}$ = .056). Additional significant results were found for the motor response templates in left M1 (z = 4.26, p < .001, $p_{corrected}$ < .001), SMA (z = 3.69, p < .001, $p_{corrected}$ < .001) and PMd (z = 2.85, p = .002, $p_{corrected}$ = .018).

Stimulus-related analyses

We further aimed to address whether the canonical templates obtained during the perception of the instructed stimuli were reactivated during the novel mappings' preparation. To do so, we followed the same procedure as in the response-related analyses, using templates built from the stimulus category localizer data. The results are displayed in **Fig. 5D** and **Fig. 5-3**. The paired-sample Wilcoxon tests were significant in all the regions explored, i.e., in V1, V2-4, LOC, and VentralVisual. Nonetheless, we did not find above-zero beta coefficients linked to relevant templates in either region. Instead, the effect was driven by below-zero beta weights associated with the irrelevant templates. The latter effect was significant in the V2-4, LOC, and VentralVIsual ROIs. In these analyses, no effects were detected in the control ROI, M1.

Since the behavioral analyses showed that one of the mappings' stimulus category conditions (the [bird-fish] combination) was linked to generally impoverished performance, we further explored the template tracking findings across conditions to ensure that the unexpected, below-zero irrelevant beta weights were not driven by an outlier pair of categories. Nonetheless, the pattern found in the main results seemed stable across

780 mappings' conditions and ROIs (**Fig. 5-6**), suggesting that these findings were not driven by
781 trials from a particular condition.

782 *Whole-brain searchlight*

783 To complement the ROIs' results, we carried out an exploratory searchlight analysis. That
784 provided whole-brain maps displaying regions where the beta weights were higher for
785 relevant than irrelevant canonical templates. The results, displayed in **Fig. 5E**, overlapped
786 substantially with the two sets of ROIs selected a priori for this work. When the motor
787 response localizer templates were used, we found a wide, bilateral cluster ([32, -14, 56], k
788 = 27155, T(1,29) = 17.21, $p < .001$) which covered the motor cortices (M1, PMd and SMA),
789 S1, the IPL and SPL, and the posterior insula. The cluster also extended into the precuneus.
790 A second cluster ([0, -62, -20], k = 5390, T(1,29) = 10.92, $p < .001$) covered the cerebellum
791 bilaterally. Regarding the action effects, we found a significant cluster ([44, -22, 58], k =
792 13826, T(1,26) = 8.29, $p < .001$) covering the SMA and the right M1 and PMd, and extended
793 into the right S1, IPL, SPL and pInsula. A second cluster involved the left S1, IPL and SPL
794 ([-52, -24, 50], k = 1200, T(1,26) = 4.69, $p = .027$). A significant cluster was also found in the
795 cerebellum ([-20, -60, -26], k = 1718, T(1,26) = 5.18, $p = .01$). Finally, the stimulus category
796 whole-brain map included a significant, bilateral cluster ([50, -76, -2], k = 12470, T(1,29) =
797 15.21, $p < .001$) extending from the early visual cortices into the fusiform gyrus and the
798 inferotemporal cortex, and which also covered part of the LOC.

799 To formally address the overlap between the canonical template tracking whole-brain maps
800 and the regions that showed a univariate signal increase during the preparation, we
801 performed three additional conjunction tests, one per localizer task. Overall, these results
802 converged in the anatomical independence between the above-described univariate and
803 multivariate preparatory signals. The motor response map overlapped with the univariate
804 results only in a restricted cluster located in the IPL ([40, -44, 45], k = 64). The same IPL

805 cluster was identified when using the action effect brain map ([41, -44, 45], k = 73), where a
806 small cluster was also found in the posterior section of the pre-SMA ([4, 9, 57], k = 21). In
807 both cases, the conjunction maps clusters covered an infimal proportion of the significant
808 voxels identified with the template tracking procedure (0.24% and 0.56%, respectively). No
809 conjunction clusters were found when using the stimulus category brain map.

810 *Control analysis: template reliability*

811 We aimed to ensure that our results were not biased by differences in reliability across the
812 canonical templates. To do so, we computed and compared (using repeated measures
813 ANOVAs) the SNR and the correlationability across the four template conditions from each
814 localizer. This analysis was carried out, separately, for each of the ROIs explored in the main
815 analysis. In general terms, these results supported that these two reliability measurements
816 were equivalent across template conditions (**Fig. 7**). We only found significant differences
817 regarding the SNR in action effect templates in the IPL, $F(3, 78) = 2.85$, $p < .043$, $\eta^2_p = .099$,
818 driven by greater SNR in the right index templates than the right middle finger template. The
819 fact that no other significant result was found in the remaining 67 tests (even when no
820 statistical correction for multiple comparisons was applied) strongly suggests that the
821 findings here reported were not contaminated by differences in the templates' reliability.

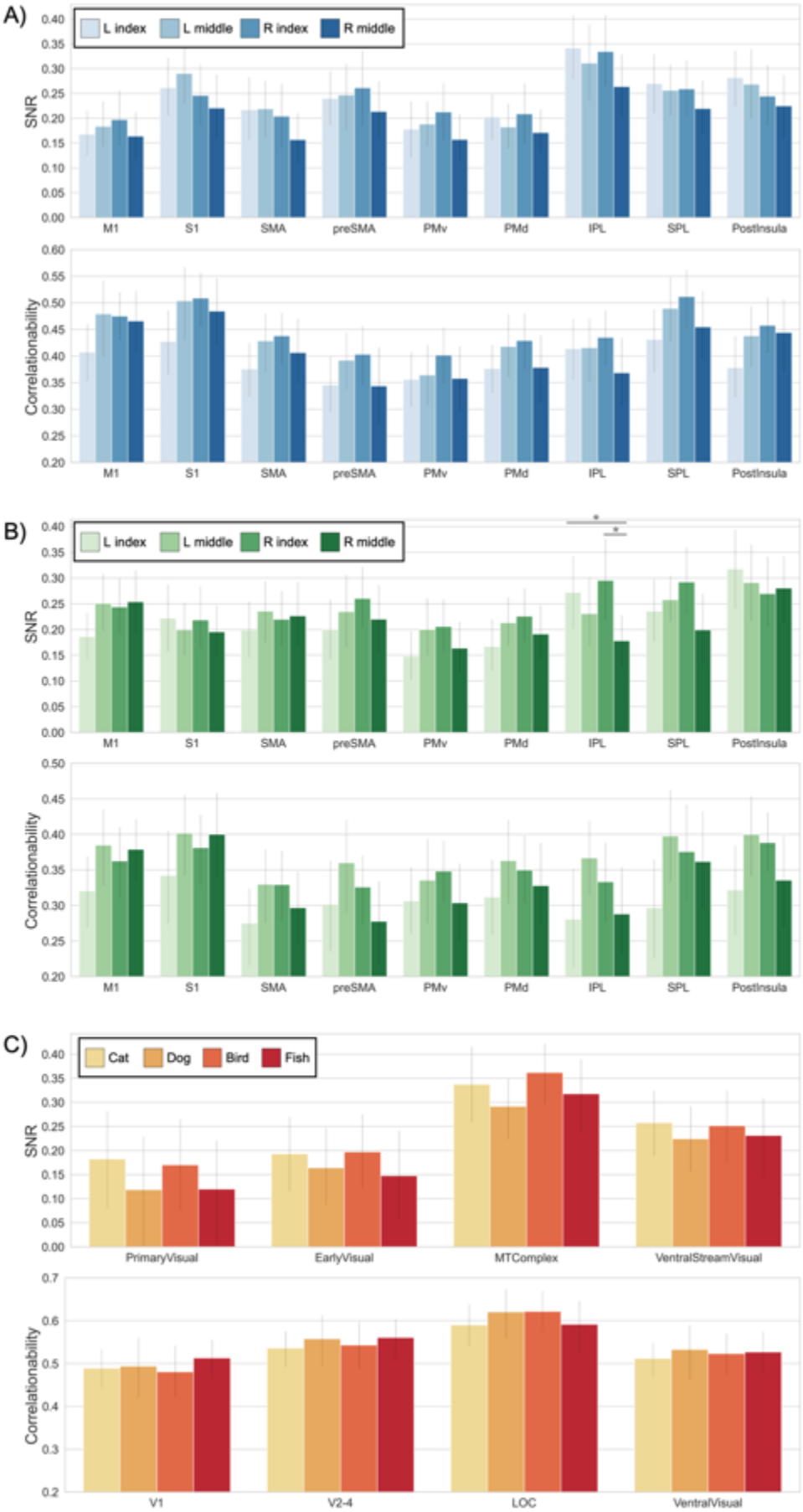

822 **Figure 7**. Canonical templates' reliability measurements (SNR, correlationability) for the motor

823 response (A), action effects (B), and stimuli category (C) templates, across ROIs. Asterisks denote
824 statistically significant differences ($p < .05$).

825 **4. Discussion**

826 In this work, we aimed to characterize the preparatory neural states leading to novel S-R
827 mapping execution. In contrast to previous literature, which has focused on abstract task-
828 level representations in MDN regions, here we addressed the contribution of lower-level
829 stimulus and response coding across the sensorimotor systems. Critically, we aimed to
830 detect activity patterns with a shared encoding format between novel mapping preparation
831 and overt performance. Using canonical template tracking, we isolated the mappings'
832 relevant sensorimotor activity patterns and estimated their representational strength during
833 task preparation. Our findings showed that the response-related components were indeed
834 pre-activated during novel mapping preparation, entailing the presence of templates that
835 captured both motor responses and their somatosensory consequences. Nonetheless, we
836 obtained less interpretable results regarding the stimulus-related templates, with non-
837 relevant stimulus representations displaying systematically smaller, below-zero similarity
838 estimates, while the representational strength of the relevant categories did not differ from
839 zero. Overall, our findings support that novel instruction preparation anticipates prospective
840 motor and kinesthetic representations while leaving open the role of stimulus neural codes.

841 Our work revealed that the encoding of response-related templates was a rather widespread
842 phenomenon across regions previously associated with action control (Haggard, 2008;
843 Rizzolatti & Luppino, 2001), detecting this effect in M1, SMA, PMd, S1, IPL, SPL, and the
844 posterior insula. These regions were not engaged in a univariate fashion during the
845 preparation, pointing out that their anticipatory recruitment did not rely on mean signal
846 increases. On the contrary, we could not evidence template instantiation in the only ROI
847 showing preparatory univariate activation (the pre-SMA). This set of frontoparietal regions

not only encoded diverse sensorimotor information (motor responses and action) but also seemed to anticipate, simultaneously, pairs of prospective action plans. In this regard, we replicated our main effects when the analyses were restricted to responses that were prepared but not executed. That also ensured that our findings were not contaminated by response-specific activity originated during task execution. Critically, beyond this overall engagement of the action control system, the evidence also highlighted the role of two areas, M1 and S1, that showed numerically larger and more consistent effects. In both, we found robust above-zero representational strengths for the relevant templates, accompanied by below-zero values for irrelevant ones. We further showed that response effector information was retained after removing the impact of laterality, stressing the specificity of representations held in these areas. Overall, our results stressed the relevance of downstream processing, especially in M1 and S1, during higher-level novel task preparation. Furthermore, we evidenced that these regions' encoding space was shared with sensorimotor execution, offering a deeper insight into their representational format (Kriegeskorte & Kievit, 2013).

Taken together, these findings fit well within the predictions of simulation-based frameworks (Grush, 2004; Jeannerod, 1994, 2001), suggesting that the task-relevant sensorimotor processing was internally anticipated before the execution. Following previous theoretical (Brass et al., 2017; Moran & O'Shea, 2020) and empirical work (Liefooghe et al., 2021; Theeuwes et al., 2018), we could interpret our results as reflecting the involvement of motor imagery when preparing for novel tasks. In this regard, recent behavioral evidence showed that novel task preparation relied on the pre-activation of effector-specific response representations, since blocking their access (via dual-task demands) robustly impaired performance (Palenciano et al., 2021). Our results seem to capture the neural mechanism underpinning that behavioral effect, evidencing the presence of low-level response

representations, and further characterizing the different action-related information that could be anticipated via motor simulation. Also supporting this view, the regions that showed anticipatory template instantiation have been linked to motor imagery in the past (Hardwick et al., 2018; Hétu et al., 2013). Moreover, some of them encode movements in a common representational space that generalizes between imagery and overt execution (Zabicki et al., 2017), as we found in our data. Nonetheless, we can alternatively interpret our findings from broader frameworks on action control. There, it has been widely documented how the somatomotor system encodes prepared actions before their execution (e.g., Gallivan, Adam McLean, et al., 2011; Gallivan, McLean, et al., 2011). Critically, and parallelizing our findings, recent data have supported a representational overlap between motor planning and execution in M1 and S1 (Ariani et al., 2020). From this view, our results could reflect that, in general terms, preparatory signals push the primary somatomotor cortices closer to execution-induced states (Churchland et al., 2010; Shenoy et al., 2013), facilitating performance. However, there is a key difference between this literature and our research: while these studies investigated how a single action is planned, we focused on the preparation of pairs of equally probable actions. Hence, our findings could help expand these models, showing how several action plans can be anticipated in parallel, to be later selected in a goal-oriented fashion (Cisek & Kalaska, 2010).

Our findings also highlighted the role of task-relevant action effects (in this case, their somatosensory consequences) during instruction preparation. This result is highly relevant for theoretical frameworks based on ideomotor principles, emphasizing that action planning is the consequence of pre-activating the intended perceptual effects (Hommel, 2009; Hommel et al., 2001; Shin et al., 2010). Agreeing with this view and previous neuroimaging findings (Waszak et al., 2012), we showed that task-relevant kinesthetic outputs were anticipated before mapping execution. Nonetheless, our work extended this research by

identifying finer-grained action effect representations, and more critically, by evidencing this effect for the first time in more volatile, novel task scenarios. Furthermore, we showed that the motor response and action effects templates captured independent facets of the preparatory activity patterns. This result is less straightforward to interpret from the above-mentioned ideomotor perspective, which would predict a greater overlap between both sets of templates. In opposition, our findings could reflect that information about the motor responses and their kinesthetic consequences may be segregated and multiplexed across these regions' representational spaces. Alternatively, they could reflect that each set of templates could also contain non-shared response information. For instance, the response templates could capture additional proprioceptive information beyond the tactile feedback. Future research will be key to describing in greater detail the nature of these representations as well as their functional role during preparation.

Contrary to the response-related results, we obtained a less clear pattern regarding the stimulus templates. We found the expected relationship between prepared and non-prepared target categories, with smaller representational strength for the latter than the former. ROI and whole-brain analyses showed that this pattern spread across the visual stream, with numerically greater effects in higher-order areas sensitive to abstract category information, such as the LOC (Grill-Spector et al., 1999). However, while the irrelevant category templates were consistently linked to negative estimates, the relevant ones were not statistically different from zero. While this finding may relate to the nature of visual imagery (which may differ from the motor domain), we believe that this pattern could be driven by the design of the category localizer task. Since participants responded to the broader animate-inanimate distinction, the individual templates' animal categories remained task-irrelevant. Although this decision allowed isolating the stimulus processing from unwanted motor confounds, it may have hindered the category information conveyed by the

923 templates. Having said that, the consistent results linked to the irrelevant templates suggest
924 that this information was somehow anticipated. Although it could be tempting to interpret this
925 finding as the suppression of irrelevant category representations during preparation, the
926 similarity measurements computed (i.e., non-cross-validated; Walther et al., 2016) require
927 that relative instead of absolute activation estimates are considered (Palenciano et al., 2022;
928 Walther et al., 2016). Hence, no inference should be performed based only on the irrelevant
929 categories' below-zero representational strength. Instead, we encourage caution when
930 interpreting these results and emphasize that more compelling evidence is required to
931 understand the significance of stimulus-related representations in this context.

932 Overall, our results highlighted the action-oriented nature of proactive novel task control,
933 and more specifically, the involvement of downstream motor and somatosensory regions.
934 This view could seem in conflict with previous literature which has stressed the role of
935 cognitive control-related MDN areas during novel instruction processing (Cole et al., 2010;
936 Demanet et al., 2016; Dumontheil et al., 2011; Hartstra et al., 2011, 2012; Palenciano,
937 González-García, Arco, & Ruz, 2019; Ruge & Wolfensteller, 2010). Therefore, the main
938 frameworks explaining instructed performance have focused on how these frontoparietal
939 regions flexibly generate task representation from scratch (Brass et al., 2009, 2017; Cole,
940 Laurent, et al., 2013). We also supported this notion, showing heightened activity during
941 mapping preparation across the MDN. Nonetheless, our methodology enabled us to identify
942 a co-existent preparatory mechanism outside this network and anchored in lower-level
943 cortices. We believe that our findings reflect a different but complementary facet of novel
944 task processing that entails the anticipatory tuning of sensorimotor systems via motor and
945 kinesthetic template instantiation. In this regard, our results left open a key question: how
946 do the higher-order task representations in the MDN, and the sensorimotor coding here
947 described, interact? Current working memory models state that abstract, multidimensional

948 representations held in the MDN (especially, in the lateral prefrontal cortex) lead to the
949 activation of more specific content encoded in the sensory regions (Christophel et al., 2017;
950 Curtis & D'Esposito, 2003; Sreenivasan et al., 2014). Following this framework, one could
951 expect that instruction representations previously found in the MDN precede and influence
952 the engagement of the concrete sensorimotor templates here reported. Future studies
953 exploiting temporally resolved brain data will be crucial to address this hypothesis and bridge
954 both sets of findings. That would enrich the current understanding of instruction processing,
955 and more generally, help to build more holistic frameworks of anticipatory task control that
956 integrate higher-order and downstream cognitive processes.

957 **5. Conclusions**

958 In this work, we addressed whether novel S-R mapping preparation entailed the pre-
959 activation of sensorimotor representations that overlapped with those guiding task
960 execution. By combining fMRI recording and tailored pattern analyses, we evidenced the
961 anticipatory engagement of templates conveying the mappings' motor responses and their
962 perceptual consequences. While this effect was widespread across frontoparietal regions
963 linked to action control, it was particularly robust in the primary somatosensory and motor
964 cortices. In contrast, we did not obtain evidence supporting an equivalent pattern regarding
965 stimulus-related perceptual templates. Overall, our findings stress that motoric and
966 kinesthetic representations anchored in the sensorimotor systems are proactively engaged
967 by instructions, suggesting that motor imagery may underpin preparation in novel contexts.
968 More broadly, these results suggest that the anticipatory and flexible tuning of the
969 sensorimotor interface systems could be a key component for current models of cognitive
970 control.

Credit author statement

AFP: Conceptualization, Methodology, Data collection, Data analysis, Writing - original draft, Writing - review & editing. CG-G: Conceptualization, Methodology, Writing - review & editing. JDH: Conceptualization, Writing - review & editing, Funding acquisition. BL: Conceptualization, Writing - review & editing, Funding acquisition. MB: Conceptualization, Writing - review & editing, Funding acquisition.

Data and code Accessibility

The raw fMRI BIDS dataset is available in the following OpenNeuro repository: https://openneuro.org/datasets/ds004829. The processed individual and group-level MRI and behavioral data, together with the scripts used for data analyses, are available on OSF: https://osf.io/dq6v5/. Group-level whole-brain maps can be also accessed in the following NeuroVault repository: https://neurovault.org/collections/XQFLCDUH/

References

Arco, J. E., González-García, C., Díaz-Gutiérrez, P., Ramírez, J., & Ruz, M. (2018). Influence of activation pattern estimates and statistical significance tests in fMRI decoding analysis. *Journal of Neuroscience Methods*, *308*, 248–260. https://doi.org/10.1016/j.jneumeth.2018.06.017

Ariani, G., Pruszynski, J. A., & Diedrichsen, J. (2022). Motor planning brings human primary somatosensory cortex into action-specific preparatory states. *ELife*, *11*. https://doi.org/10.7554/ELIFE.69517

Bourguignon, N. J., Braem, S., Hartstra, E., De Houwer, J., & Brass, M. (2018). Encoding of Novel Verbal Instructions for Prospective Action in the Lateral Prefrontal Cortex: Evidence from Univariate and Multivariate Functional Magnetic Resonance Imaging

Analysis. *Journal of Cognitive Neurosciencen*, *30*(8), 1170–1184. https://doi.org/10.1162/jocn

Brady, T. F., Konkle, T., Alvarez, G. A., & Oliva, A. (2013). Real-world objects are not represented as bound units: Independent forgetting of different object details from visual memory. *Journal of Experimental Psychology: General*, *142*(3), 791–808. https://doi.org/10.1037/A0029649

Brass, M., Liefooghe, B., Braem, S., & de Houwer, J. (2017). Following new task instructions: Evidence for a dissociation between knowing and doing. *Neuroscience & Biobehavioral Reviews*, *81*, 16–28. https://linkinghub.elsevier.com/retrieve/pii/S0149763416306856

Brass, M., Wenke, D., Spengler, S., & Waszak, F. (2009). Neural correlates of overcoming interference from instructed and implemented stimulus-response associations. *Journal of Neuroscience*, *29*(6), 1766–1772. https://doi.org/10.1523/JNEUROSCI.5259-08.2009

Brodeur, M. B., Guérard, K., & Bouras, M. (2014). Bank of Standardized Stimuli (BOSS) Phase II: 930 New Normative Photos. *PLOS ONE*, *9*(9), e106953. https://doi.org/10.1371/JOURNAL.PONE.0106953

Christophel, T. B., Klink, P. C., Spitzer, B., Roelfsema, P. R., & Haynes, J.-D. (2017). The Distributed Nature of Working Memory. *Trends in Cognitive Sciences*, *21*(2), 111–124. https://doi.org/10.1016/j.tics.2016.12.007

Churchland, M. M., Cunningham, J. P., Kaufman, M. T., Ryu, S. I., & Shenoy, K. V. (2010). Cortical Preparatory Activity: Representation of Movement or First Cog in a Dynamical Machine? *Neuron*, *68*(3), 387–400. https://doi.org/10.1016/J.NEURON.2010.09.015

Cisek, P., & Kalaska, J. F. (2010). Neural Mechanisms for Interacting with a World Full of Action Choices. *Annual Review of Neuroscience*, *33*(1), 269–298. https://doi.org/10.1146/annurev.neuro.051508.135409

Cole, M. W., Bagic, A., Kass, R., & Schneider, W. (2010). Prefrontal Dynamics Underlying Rapid Instructed Task Learning Reverse with Practice. *Journal of Neuroscience*, *30*(42), 14245–14254. https://doi.org/10.1523/JNEUROSCI.1662-10.2010

Cole, M. W., Etzel, J. A., Zacks, J. M., Schneider, W., & Braver, T. S. (2011). Rapid Transfer of Abstract Rules to Novel Contexts in Human Lateral Prefrontal Cortex. *Frontiers in Human Neuroscience*, *5*(November), 1–13. https://doi.org/10.3389/fnhum.2011.00142

Cole, M. W., Laurent, P., & Stocco, A. (2013). Rapid instructed task learning: A new window into the human brain's unique capacity for flexible cognitive control. *Cognitive, Affective and Behavioral Neuroscience*, *13*(1), 1–22. https://doi.org/10.3758/s13415-012-0125-7

Cole, M. W., Reynolds, J. R., Power, J. D., Repovs, G., Anticevic, A., & Braver, T. S. (2013). Multi-task connectivity reveals flexible hubs for adaptive task control. *Nature Neuroscience*, *16*(9), 1348–1355. https://doi.org/10.1038/nn.3470

Curtis, C. E., & D'Esposito, M. (2003). Persistent activity in the prefrontal cortex during working memory. *Trends in Cognitive Sciences*, *7*(9), 415–423. https://doi.org/10.1016/S1364-6613(03)00197-9

Demanet, J., Liefooghe, B., Hartstra, E., Wenke, D., De Houwer, J., & Brass, M. (2016). There is more into 'doing' than 'knowing': The function of the right inferior frontal sulcus is specific for implementing versus memorising verbal instructions. *NeuroImage*, *141*, 350–356. https://doi.org/10.1016/j.neuroimage.2016.07.059

Dumontheil, I., Thompson, R., & Duncan, J. (2011). Assembly and Use of New Task Rules in Fronto-parietal Cortex. *Journal of Cognitive Neuroscience*, *23*(1), 168–182. https://doi.org/10.1162/jocn.2010.21439

Duncan, J. (2010). The multiple-demand (MD) system of the primate brain: mental programs for intelligent behaviour. *Trends in Cognitive Sciences*, *14*(4), 172–179. https://doi.org/10.1016/j.tics.2010.01.004

Everaert, T., Theeuwes, M., Liefooghe, B., & De Houwer, J. (2014). Automatic Motor Activation by Mere Instruction. *Cognitive, Affective and Behavioral Neuroscience*, *14*, 1300–1309. https://doi.org/10.3758/s13415-014-0294-7

Fedorenko, E., Duncan, J., & Kanwisher, N. (2013). Broad domain generality in focal regions of frontal and parietal cortex. *Proceedings of the National Academy of Sciences of the United States of America*, *110*(41), 16616–16621. https://doi.org/10.1073/pnas.1315235110

Gallivan, J. P., Adam McLean, D., Smith, F. W., & Culham, J. C. (2011). Decoding Effector-Dependent and Effector-Independent Movement Intentions from Human Parieto-Frontal Brain Activity. *Journal of Neuroscience*, *31*(47), 17149–17168. https://doi.org/10.1523/JNEUROSCI.1058-11.2011

Gallivan, J. P., McLean, D. A., Valyear, K. F., Pettypiece, C. E., & Culham, J. C. (2011). Decoding Action Intentions from Preparatory Brain Activity in Human Parieto-Frontal Networks. *Journal of Neuroscience*, *31*(26), 9599–9610. https://doi.org/10.1523/JNEUROSCI.0080-11.2011

Glasser, M. F., Coalson, T. S., Robinson, E. C., Hacker, C. D., Harwell, J., Yacoub, E., Ugurbil, K., Andersson, J., Beckmann, C. F., Jenkinson, M., Smith, S. M., & Van Essen,

D. C. (2016). A multi-modal parcellation of human cerebral cortex. *Nature*, *536*(7615), 171–178. https://doi.org/10.1038/nature18933

González-García, C., Arco, J. E., Palenciano, A. F., Ramírez, J., & Ruz, M. (2017). Encoding, preparation and implementation of novel complex verbal instructions. *NeuroImage*, *148*, 264–273. https://doi.org/10.1016/J.NEUROIMAGE.2017.01.037

González-García, C., Formica, S., Liefooghe, B., & Brass, M. (2020). Attentional prioritization reconfigures novel instructions into action-oriented task sets. *Cognition*, *194*. https://doi.org/10.1016/j.cognition.2019.104059

González-García, C., Formica, S., Wisniewski, D., & Brass, M. (2021). Frontoparietal action-oriented codes support novel instruction implementation. *NeuroImage*, *226*, 117608. https://doi.org/10.1016/j.neuroimage.2020.117608

Gratton, G., Coles, M. G., Sirevaag, E. J., Eriksen, C. W., & et al. (1988). Pre- and poststimulus activation of response channels: a psychophysiological analysis. *Journal of Experimental Psychology. Human Perception and Performance*, *14*(3), 331–344. https://doi.org/10.1037//0096-1523.14.3.331

Griffin, G., Holub, A., & Perona, P. (2007). *Caltech-256 Object Category Dataset*. https://resolver.caltech.edu/CaltechAUTHORS:CNS-TR-2007-001

Grill-Spector, K., Kushnir, T., Edelman, S., Avidan, G., Itzchak, Y., & Malach, R. (1999). Differential processing of objects under various viewing conditions in the human lateral occipital complex. *Neuron*, *24*(1), 187–203. https://doi.org/10.1016/S0896-6273(00)80832-6

Grush, R. (2004). The emulation theory of representation: Motor control, imagery, and perception. *Behavioral and Brain Sciences*, *27*(3), 377–396. https://doi.org/10.1017/S0140525X04000093

Guillot, A., & Collet, C. (2005). Contribution from neurophysiological and psychological methods to the study of motor imagery. In *Brain Research Reviews* (Vol. 50, Issue 2, pp. 387–397). Elsevier. https://doi.org/10.1016/j.brainresrev.2005.09.004

Haggard, P. (2008). Human volition: towards a neuroscience of will. *Nature Reviews Neuroscience 2008 9:12*, *9*(12), 934–946. https://doi.org/10.1038/nrn2497

Hardwick, R. M., Caspers, S., Eickhoff, S. B., & Swinnen, S. P. (2018). Neural correlates of action: Comparing meta-analyses of imagery, observation, and execution. In *Neuroscience and Biobehavioral Reviews* (Vol. 94, pp. 31–44). Elsevier Ltd. https://doi.org/10.1016/j.neubiorev.2018.08.003

Hartstra, E., Kühn, S., Verguts, T., & Brass, M. (2011). The implementation of verbal instructions: An fMRI study. *Human Brain Mapping*, *32*(11), 1811–1824. https://doi.org/10.1002/hbm.21152

Hartstra, E., Waszak, F., & Brass, M. (2012). The implementation of verbal instructions: Dissociating motor preparation from the formation of stimulus-response associations. *NeuroImage*, *63*(3), 1143–1153. https://doi.org/10.1016/j.neuroimage.2012.08.003

Hétu, S., Grégoire, M., Saimpont, A., Coll, M. P., Eugène, F., Michon, P. E., & Jackson, P. L. (2013). The neural network of motor imagery: An ALE meta-analysis. In *Neuroscience and Biobehavioral Reviews* (Vol. 37, Issue 5, pp. 930–949). Pergamon. https://doi.org/10.1016/j.neubiorev.2013.03.017

Hommel, B. (2009). Action control according to TEC (theory of event coding). *Psychological Research*, *73*(4), 512–526. https://doi.org/10.1007/s00426-009-0234-2

Hommel, B., Müsseler, J., Aschersleben, G., & Prinz, W. (2001). The Theory of Event Coding (TEC): A framework for perception and action planning. *Behavioral and Brain Sciences*, *24*(5), 849–878. https://doi.org/10.1017/S0140525X01000103

Jeannerod, M. (1994). The representing brain: neural correlates of motor intention and imagery. *Behavioral and Brain Sciences*, *17*(2), 187–245. http://www.bbsonline.org/documents/a/00/00/05/35/bbs00000535-00/b...

Jeannerod, M. (2001). Neural simulation of action: A unifying mechanism for motor cognition. *NeuroImage*, *14*(1), S103–S109. https://doi.org/10.1006/nimg.2001.0832

Konkle, T., Brady, T. F., Alvarez, G. A., & Oliva, A. (2010). Conceptual distinctiveness supports detailed visual long-term memory for real-world objects. *Journal of Experimental Psychology: General*, *139*(3), 558–578. https://doi.org/10.1037/A0019165

Kriegeskorte, N., & Kievit, R. A. (2013). Representational geometry: Integrating cognition, computation, and the brain. In *Trends in Cognitive Sciences* (Vol. 17, Issue 8, pp. 401–412). https://doi.org/10.1016/j.tics.2013.06.007

Kriegeskorte, N., Mur, M., & Bandettini, P. (2008). Representational similarity analysis – connecting the branches of systems neuroscience. *Frontiers in Systems Neuroscience*, *2*, 4. https://doi.org/10.3389/neuro.06.004.2008

Liefooghe, B., & De Houwer, J. (2018). Automatic effects of instructions do not require the intention to execute these instructions. *Journal of Cognitive Psychology*, *30*(1), 108–121. https://doi.org/10.1080/20445911.2017.1365871

Liefooghe, B., De Houwer, J., & Wenke, D. (2013). Instruction-based response activation depends on task preparation. *Psychonomic Bulletin and Review*, *20*(3), 481–487. https://doi.org/10.3758/s13423-013-0374-7

Liefooghe, B., Jim, A., & De Houwer, J. (2021). Automatic effects of covert practice. *Quarterly Journal of Experimental Psychology (2006)*, 17470218211007138. https://doi.org/10.1177/17470218211007138

Liefooghe, B., Wenke, D., & De Houwer, J. (2012). Instruction-based task-rule congruency effects. *Journal of Experimental Psychology: Learning, Memory, and Cognition*, *38*(5), 1325–1335. https://doi.org/10.1037/a0028148

Mayka, M. A., Corcos, D. M., Leurgans, S. E., & Vaillancourt, D. E. (2006). Three-dimensional locations and boundaries of motor and premotor cortices as defined by functional brain imaging: a meta-analysis. *NeuroImage*, *31*(4), 1453–1474. https://doi.org/10.1016/J.NEUROIMAGE.2006.02.004

Meiran, N., & Cohen-Kdoshay, O. (2012). Working memory load but not multitasking eliminates the prepared reflex: Further evidence from the adapted flanker paradigm. *Acta Psychologica*, *139*(2), 309–313. https://doi.org/10.1016/j.actpsy.2011.12.008

Meiran, N., Pereg, M., Kessler, Y., Cole, M. W., & Braver, T. S. (2015a). Reflexive activation of newly instructed stimulus–response rules: evidence from lateralized readiness potentials in no-go trials. *Cognitive, Affective and Behavioral Neuroscience*, *15*(2), 365–373. https://doi.org/10.3758/s13415-014-0321-8

Meiran, N., Pereg, M., Kessler, Y., Cole, M. W., & Braver, T. S. (2015b). The power of instructions: Proactive configuration of stimulus–response translation. *Journal of Experimental Psychology: Learning, Memory, and Cognition*, *41*(3), 768–786. https://doi.org/10.1037/xlm0000063

Moran, A., & O'Shea, H. (2020). Motor Imagery Practice and Cognitive Processes. *Frontiers in Psychology*, *11*(March). https://doi.org/10.3389/fpsyg.2020.00394

Muhle-Karbe, P. S., Duncan, J., De Baene, W., Mitchell, D. J., & Brass, M. (2017). Neural Coding for Instruction-Based Task Sets in Human Frontoparietal and Visual Cortex. *Cerebral Cortex*, *27*(3), 1891–1905. https://doi.org/10.1093/cercor/bhw032

Mumford, J. A., Davis, T., & Poldrack, R. A. (2014). The impact of study design on pattern estimation for single-trial multivariate pattern analysis. *NeuroImage*, *103*, 130–138. https://doi.org/10.1016/J.NEUROIMAGE.2014.09.026

Mumford, J. A., Turner, B. O., Ashby, F. G., & Poldrack, R. A. (2012). Deconvolving BOLD activation in event-related designs for multivoxel pattern classification analyses. *NeuroImage*, *59*, 2636–2643. https://doi.org/10.1016/j.neuroimage.2011.08.076

Nichols, T., Brett, M., Andersson, J., Wager, T., & Poline, J. B. (2005). Valid conjunction inference with the minimum statistic. *NeuroImage*, *25*(3), 653–660. https://doi.org/10.1016/j.neuroimage.2004.12.005

Palenciano, A. F., González-García, C., Arco, J. E., Pessoa, L., & Ruz, M. (2019). Representational organization of novel task sets during proactive encoding. *Journal of Neuroscience*, 0725–19. https://doi.org/10.1523/JNEUROSCI.0725-19.2019

Palenciano, A. F., González-García, C., Arco, J. E., & Ruz, M. (2019). Transient and Sustained Control Mechanisms Supporting Novel Instructed Behavior. *Cerebral Cortex*, *29*(9), 3948–3960. https://doi.org/10.1093/cercor/bhy273

Palenciano, A. F., González-García, C., De Houwer, J., Brass, M., & Liefooghe, B. (2021). Exploring the link between novel task proceduralization and motor simulation. *Journal of Cognition*, *4*(1). https://doi.org/10.5334/JOC.190/METRICS/

Palenciano, A. F., Senoussi, M., Formica, S., & González-García, C. (2022). Canonical template tracking: measuring the activation state of specific neural representations. *Under Review.*

Palenciano, A. F., Senoussi, M., Formica, S., & González-García, C. (2023). Canonical template tracking: Measuring the activation state of specific neural representations. *Frontiers in Neuroimaging*, *1*, 52. https://doi.org/10.3389/FNIMG.2022.974927

Peirce, J., Gray, J. R., Simpson, S., MacAskill, M., Höchenberger, R., Sogo, H., Kastman, E., & Lindeløv, J. K. (2019). PsychoPy2: Experiments in behavior made easy. *Behavior Research Methods*, *51*(1), 195–203. https://doi.org/10.3758/s13428-018-01193-y

Possidónio, C., Graça, J., Piazza, J., & Prada, M. (2019). Animal Images Database: Validation of 120 Images for Human-Animal Studies. *Animals*, *9*(8), 475. https://doi.org/10.3390/ani9080475

Rizzolatti, G., & Luppino, G. (2001). The Cortical Motor System. *Neuron*, *31*(6), 889–901. https://doi.org/10.1016/S0896-6273(01)00423-8

Ruge, H., & Wolfensteller, U. (2010). Rapid formation of pragmatic rule representations in the human brain during instruction-based learning. *Cerebral Cortex*, *20*(7), 1656–1667. https://doi.org/10.1093/cercor/bhp228

Russo, N., Hagmann, C. E., Andrews, R., Black, C., Silberman, M., & Shea, N. (2018). Validation of the C.A.R.E. stimulus set of 640 animal pictures: Name agreement and quality ratings. *PLOS ONE*, *13*(2), e0192906. https://doi.org/10.1371/journal.pone.0192906

Shenoy, K. V., Sahani, M., & Churchland, M. M. (2013). Cortical Control of Arm Movements: A Dynamical Systems Perspective. *Https://Doi.Org/10.1146/Annurev-Neuro-062111-150509*, *36*, 337–359. https://doi.org/10.1146/ANNUREV-NEURO-062111-150509

Shin, Y. K., Proctor, R. W., & Capaldi, E. J. (2010). A Review of Contemporary Ideomotor Theory. *Psychological Bulletin*, *136*(6), 943–974. https://doi.org/10.1037/A0020541

Sreenivasan, K. K., Curtis, C. E., & D'Esposito, M. (2014). Revisiting the role of persistent neural activity during working memory. *Trends in Cognitive Sciences*, *18*(2), 82–89. https://doi.org/10.1016/j.tics.2013.12.001

Theeuwes, M., Liefooghe, B., De Schryver, M., & De Houwer, J. (2018). The role of motor imagery in learning via instructions. *Acta Psychologica*, *184*, 110–123. https://doi.org/10.1016/j.actpsy.2017.05.002

Walther, A., Nili, H., Ejaz, N., Alink, A., Kriegeskorte, N., & Diedrichsen, J. (2016). Reliability of dissimilarity measures for multi-voxel pattern analysis. *NeuroImage*, *137*, 188–200. https://doi.org/10.1016/j.neuroimage.2015.12.012

Waszak, F., Cardoso-Leite, P., & Hughes, G. (2012). Action effect anticipation: Neurophysiological basis and functional consequences. *Neuroscience & Biobehavioral Reviews*, *36*(2), 943–959. https://doi.org/10.1016/J.NEUBIOREV.2011.11.004

Zabicki, A., De Haas, B., Zentgraf, K., Stark, R., Munzert, J., & Krüger, B. (2017). Imagined and executed actions in the human motor system: Testing neural similarity between execution and imagery of actions with a multivariate approach. *Cerebral Cortex*, *27*(9), 4523–4536. https://doi.org/10.1093/cercor/bhw257

Extended data

Figure 5-1

Results from the Wilcoxon Signed-Ranked tests using the motor response and action effects templates.

	Motor response localizer									Action effects localizer								
	Relevant vs. irrelevant			*Relevant against 0*			*Irrelevant against 0*			*Relevant vs. irrelevant*			*Relevant against 0*			*Irrelevant against 0*		
	z	*p*	p_{corr}	*z*	*p*	p_{corr}	*z*	*p*	p_{corr}	*z*	*p*	p_{corr}	*z*	*p*	p_{corr}	*z*	*p*	p_{corr}
leftM1	4.78	<.001	<.001	4.72	<.001	<.001	-4.68	<.001	<.001	1.93	.026	.056	3.22	.001	.002	0.19	.848	1
rightM1	4.78	<.001	<.001	4.70	<.001	<.001	-4.78	<.001	<.001	4.02	<.001	<.001	4.40	<.001	<.001	-2.55	.011	.188
leftS1	4.78	<.001	<.001	4.76	<.001	<.001	-4.00	<.001	<.001	3.54	<.001	<.001	3.63	<.001	<.001	-1.80	.072	.201
rightS1	4.69	<.001	<.001	4.72	<.001	<.001	-4.47	<.001	<.001	4.43	<.001	<.001	4.47	<.001	<.001	-3.46	<.001	.002
SMA	4.77	<.001	<.001	4.43	<.001	<.001	-2.05	.041	.057	3.52	<.001	<.001	3.92	<.001	<.001	0.77	.442	1
preSMA	0.45	.325	.678	0.57	.572	.507	0.85	.393	1	2.01	.022	.056	1.27	.203	.258	-0.02	.980	1
PMv	0.91	.183	.678	3.40	<.001	.001	3.75	<.001	<.001	0.76	.225	.210	2.23	.025	.083	1.11	.269	1
PMd	4.26	<.001	<.001	4.45	<.001	<.001	-0.69	.491	1	3.71	<.001	<.001	3.92	<.001	<.001	0.82	.414	1
IPL	3.17	<.001	<.001	3.03	.002	.002	-0.24	.813	1	3.50	<.001	<.001	3.00	.003	.005	-0.62	.532	1
SPL	3.78	<.001	<.001	3.51	<.001	<.001	-1.55	.120	.243	2.68	.003	.003	3.82	<.001	<.001	1.61	.107	.512
pInsula	4.67	<.001	<.001	3.90	<.001	<.001	-2.52	.012	.037	4.36	<.001	<.001	3.24	.001	.006	-3.46	<.001	.002
V1	-0.82	.795	.825	-1.45	.147	.357	-0.79	.428	1	-0.28	.609	.684	1.13	.258	.394	1.58	.113	.686

Extended data

Figure 5-2

Results of the posthoc comparisons from the repeated measures ANOVA including the motor response and action effects templates simultaneously.

	Motor response			*Action effects*		
	z	*p*	p_{corr}	*z*	*p*	p_{corr}
left M1	4.53	<.001	<.001	2.51	.006	.011
right M1	4.53	<.001	<.001	4.23	<.001	<.001
left S1	4.53	<.001	<.001	3.57	<.001	<.001
right S1	4.43	<.001	<.001	4.26	<.001	<.001
SMA	4.53	<.001	<.001	3.33	<.001	<.001
preSMA	0.80	.210	.707	2.49	.006	.018
PMv	0.88	.190	.707	0.80	.210	.648
PMd	4.05	<.001	<.001	3.40	<.001	<.001
IPL	3.23	<.001	<.001	3.40	<.001	<.001
SPL	3.59	<.001	.001	2.97	.002	.004
pInsula	4.43	<.001	<.001	3.98	<.001	<.001
V1	-2.05	.775	.816	-1.36	.097	.157

Extended data

Figure 5-3

Results from the Wilcoxon Signed-Ranked tests using the stimulus category templates.

	Relevant vs. irrelevant			*Relevant against 0*			*Irrelevant against 0*		
	z	*p*	p_{corr}	*z*	*p*	p_{corr}	*z*	*p*	p_{corr}
V1	3.27	<.001	<.001	0.75	.452	.707	-2.73	.006	.012
V2-4	4.55	<.001	<.001	-1.31	.192	1	-4.64	<.001	<.001
LOC	4.77	<.001	<.001	-2.97	.039	.673	-4.78	<.001	<.001
VentralVisual	4.67	<.001	<.001	-1.24	.213	1	-4.78	<.001	<.001
M1	-0.88	.812	.590	1.08	.280	.157	1.32	.185	.252

Extended data

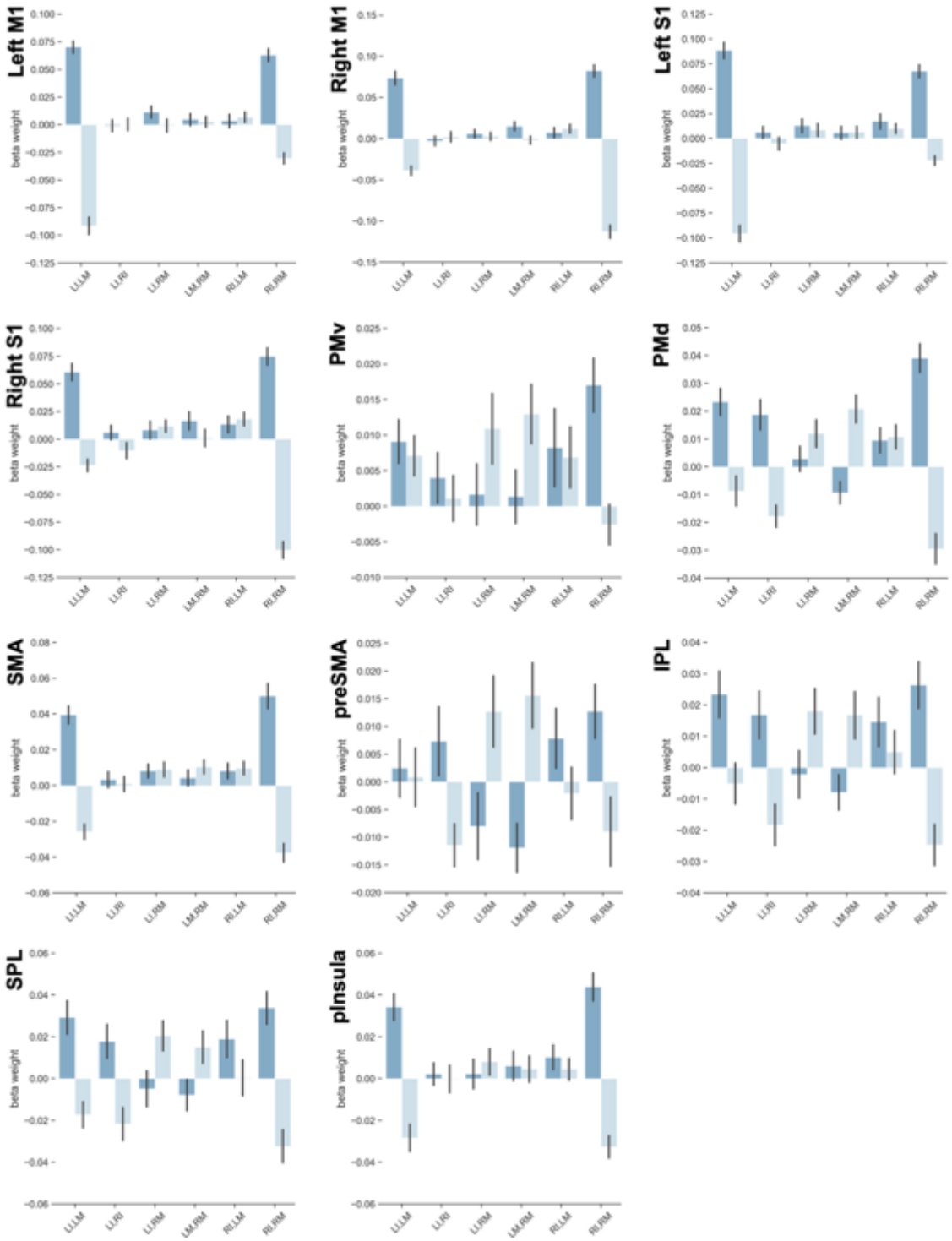

Figure 5-4. Bar plots displaying the averaged beta weight for relevant and irrelevant motor response templates, across mappings' conditions (shown in the X axes) and ROIs. These data were shown for illustrative purposes only. Hence, no statistical information is represented in this figure.

Extended data

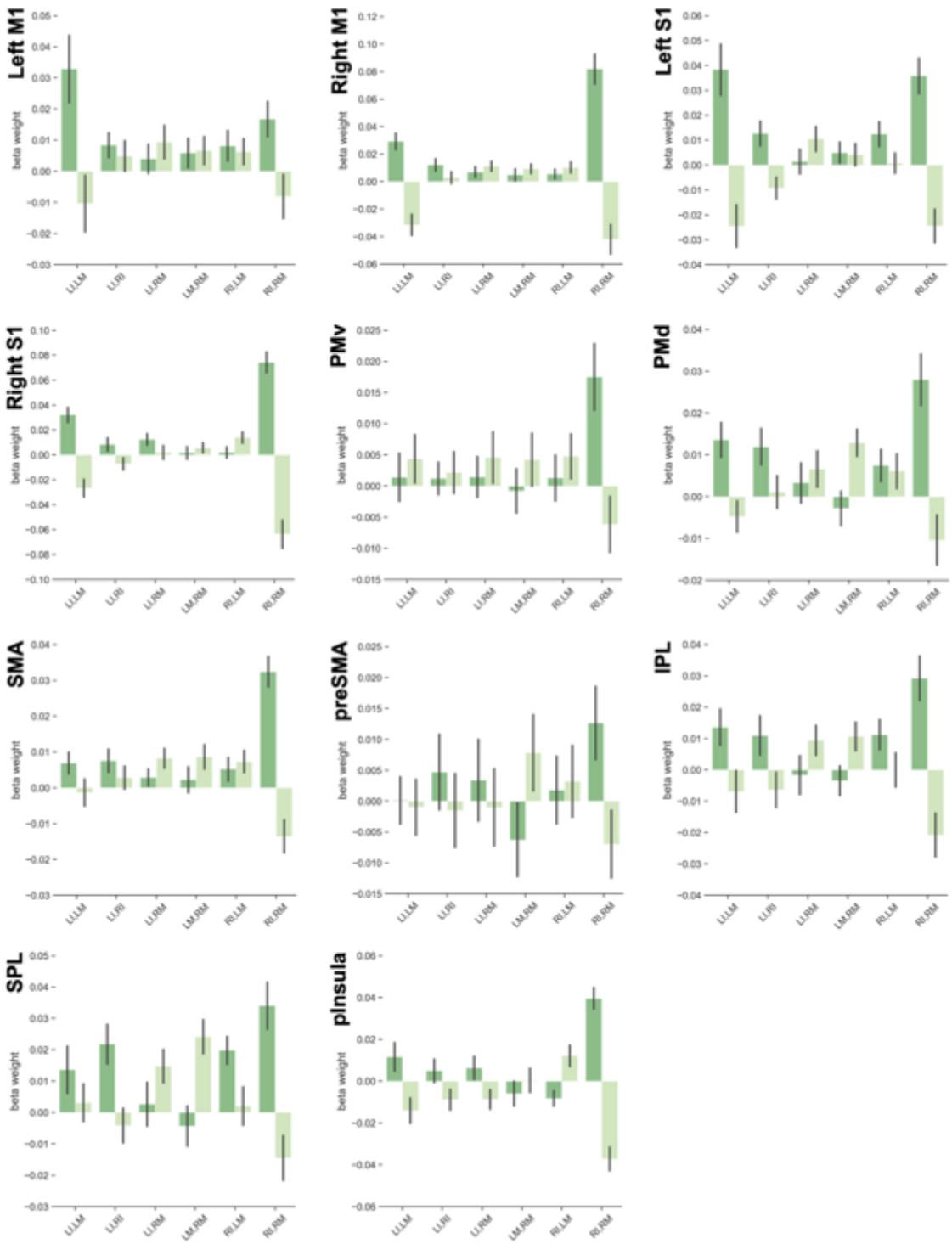

Figure 5-5. Bar plots displaying the averaged beta weight for relevant and irrelevant action effects templates, across mappings' conditions (shown in the X axes) and ROIs. These data were shown for illustrative purposes only. Hence, no statistical information is represented in this figure.

Extended data

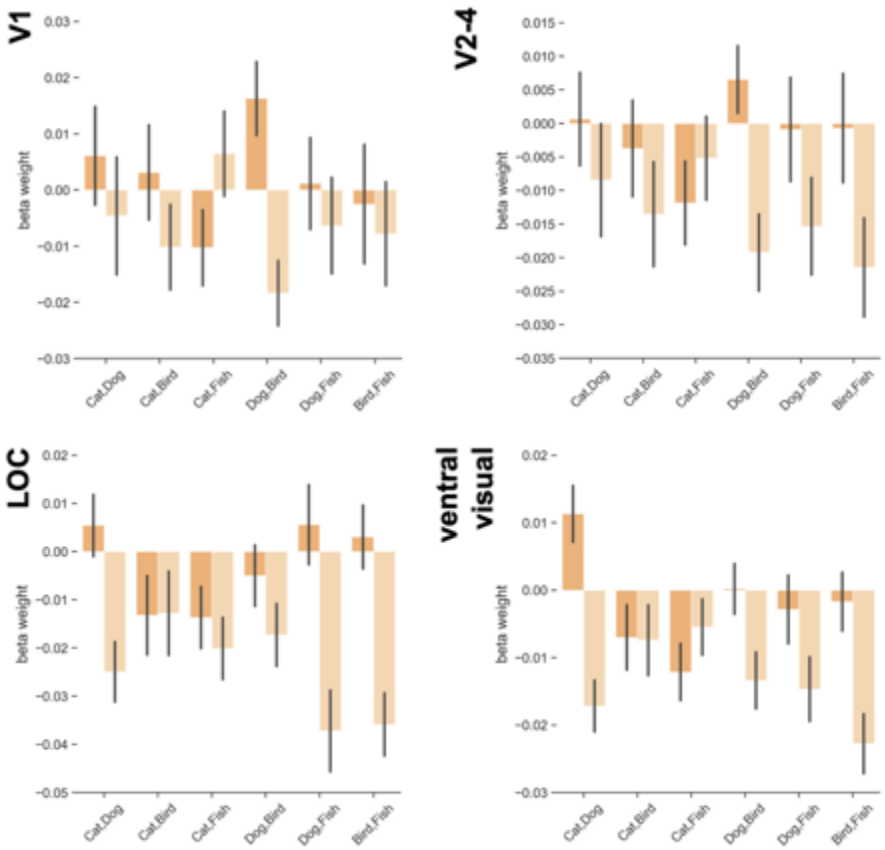

Figure 5-6. Bar plots displaying the averaged beta weight for relevant and irrelevant stimulus category templates, across mappings' conditions (shown in the X axes) and ROIs. These data were shown for illustrative purposes only. Hence, no statistical information is represented in this figure.